AD-A154 864 SCRIBE DATA OF OCTOBER 23 1983 FLIGHT(U) MASSACHUSETTS 1/1
UNIV AMHERST ASTRONOMY RESEARCH FACILITY
H SAKAI ET AL. AUG 84 UMASS-ARF-84-004 AFGL-TR-84-0208
UNCLASSIFIED F19628-84-K-0009 F/G 20/6 NL

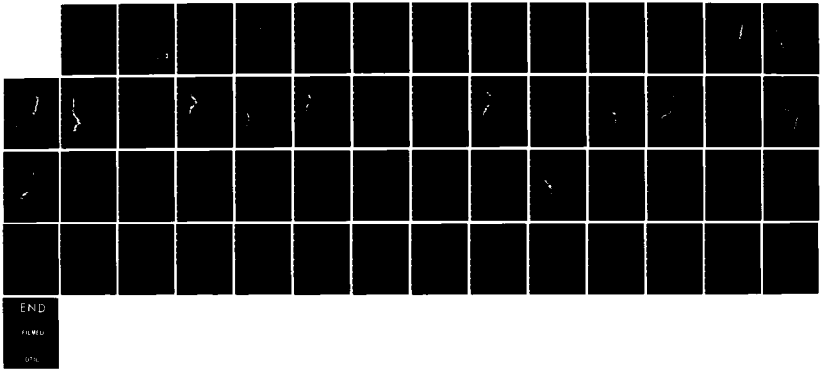

END
FILMED
DTIC

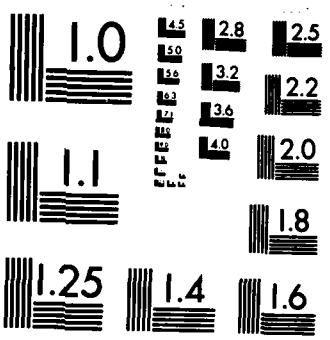

AFGL-TR-84-0208

3

SCRIBE DATA OF OCTOBER 23, 1983 FLIGHT

Hajime Sakai
George Vanasse

Astronomy Research Facility
University of Massachusetts
Amherst, Massachusetts 01003

Scientific Report No. 1

August 1984

Approved for public release; distribution unlimited

AIR FORCE GEOPHYSICS LABORATORY
AIR FORCE SYSTEMS COMMAND
UNITED STATES AIR FORCE
HANSCOM AFB, MASSACHUSETTS 01731

"This technical report has been reviewed and is approved for publication"

(Signature)

Contract Manager

(Signature)
BERTRAM D. SCHURIN
Branch Chief

FOR THE COMMANDER

(Signature)
JOHN S. GARING
Division Director

This report has been reviewed by the ESD Public Affairs Office (PA) and is releasable to the National Technical Information Service (NTIS)

Qualified requestors may obtain additional copies from the Defense Technical Information Center. All others should apply to the National Technical Information Service.

If your address has changed, or if you wish to be removed from the mailing list, or if the addressee is no longer employed by your organization, please notify AFGL/DAA, Hanscom AFB, MA 01731. This will assist us in maintaining a current mailing list.

DISCLAIMER NOTICE

THIS DOCUMENT IS BEST QUALITY PRACTICABLE. THE COPY FURNISHED TO DTIC CONTAINED A SIGNIFICANT NUMBER OF PAGES WHICH DO NOT REPRODUCE LEGIBLY.

REPORT DOCUMENTATION PAGE

READ INSTRUCTIONS BEFORE COMPLETING FORM

1. REPORT NUMBER: AFGL-TR-84-0208	2. GOVT ACCESSION NO.: AD-A154 864
3. RECIPIENT'S CATALOG NUMBER:	
4. TITLE (and Subtitle): SCRIBE Data of October 23, 1983 Flight	5. TYPE OF REPORT & PERIOD COVERED: Scientific Report No.1
	6. PERFORMING ORG. REPORT NUMBER: UMass - ARF-84-004
7. AUTHOR(s): Hajime Sakai George Vanasse *	8. CONTRACT OR GRANT NUMBER(s): F19628-84-K-0009
9. PERFORMING ORGANIZATION NAME AND ADDRESS: Astronomy Research Facility University of Massachusetts Amherst, MA 01003	10. PROGRAM ELEMENT, PROJECT, TASK AREA & WORK UNIT NUMBERS: 61102F 268801DA
11. CONTROLLING OFFICE NAME AND ADDRESS: Air Force Geophysics Laboratory Hanscom AFB, Massachusetts 01731 Monitor/Lawrence Rothman/OPI	12. REPORT DATE: August 1984 13. NUMBER OF PAGES: 52
14. MONITORING AGENCY NAME & ADDRESS (if different from Controlling Office)	15. SECURITY CLASS. (of this report): unclassified 15a. DECLASSIFICATION/DOWNGRADING SCHEDULE

16. DISTRIBUTION STATEMENT (of this Report)

Approved for public release; distribution unlimited

17. DISTRIBUTION STATEMENT (of the abstract entered in Block 20, if different from Report)

18. SUPPLEMENTARY NOTES

*AFGL/OPI, Hanscom AFB, MA 01731

19. KEY WORDS (Continue on reverse side if necessary and identify by block number)

Infrared Emission
Atmospheric Emission
Fourier Spectroscopy
Cryogenic Interferometer
CO_2 Spectrum
H_2O Spectrum
HNO_3 Spectrum

20. ABSTRACT (Continue on reverse side if necessary and identify by block number)

SCRIBE - Oct-23-1983 Interferometer data are described in this report

SCRIBE Data of October 23, 1983 Flight

Introduction

This document describes a cryogenic interferometer

SCRIBE-Oct-23-1983 interferometer was launched at 12:12 GMT from Holloman AFB ,NM . The instrument package reached the ceiling altitude at approximately 14:00. The data measurement was terminated at approximately 16:00 . The parameters pertinent to the data measurement are presented collectively in Figure 1. The on-board instrument functioned satisfactorily for most of this time period. The PCM telemetry data were found processable during this time except for a short period between 12:30 and 13:00. The interferometer sampling scheme worked satisfactorily. Only few interferogram data showed faulty sampling during the entire flight. Each interferogram scan took approximately 30 seconds covering the optical path difference range from 0 cm to its maximum value over 8.25 cm. The interferogram signals were recorded with adequate signal-to-noise ratio to warrant spectral recovery with a full spectral resolution figure of 0.060265 ~~cm^{-1}~~ /cm. Table of contents: infrared emission; atmospheric emission; fourier spectroscopy; charts; computations.

The SCRIBE instrumentation has been previously described together with the data obtained in other flights, consequently the description of the SCRIBE instrumentation will not be

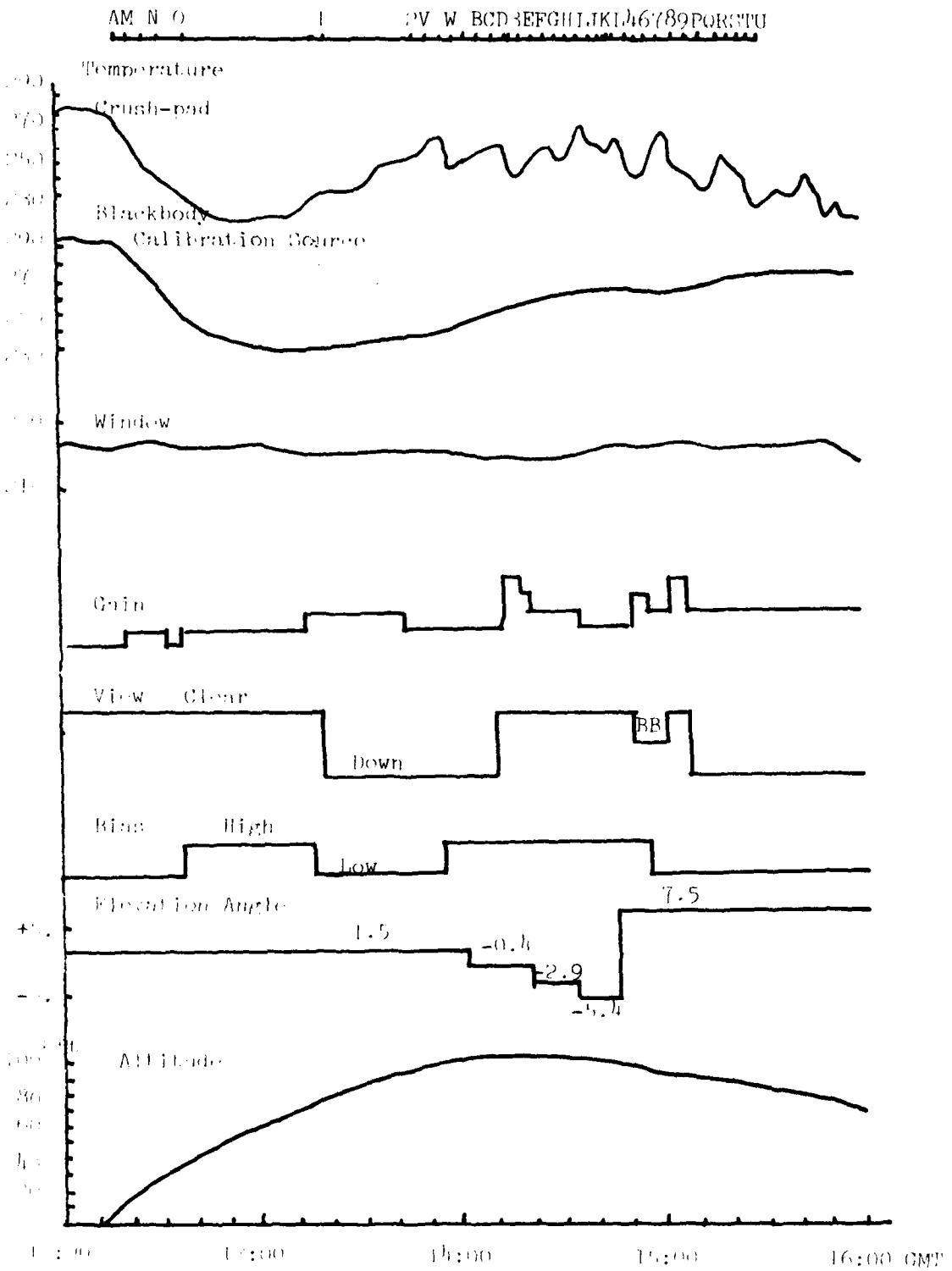
AM N O I :V W BCD3EFGHIJKL46789PQRSTU
Temperature
Crush-pad
Blackbody
Calibration Source
Window
Gain
View Clear
Down
BB
Bias High
Low
Elevation Angle
1.5
-0.4
-2.9
-5.4
7.5
Altitude
16:00 GMT

described here. [1-6]

Radiance Calibration

The emission from the on-board blackbody calibration source was observed during 14:50 to 15:00 GMT. Its temperature of 263°K was recorded by an attached thermistor thermometer during this time period. The radiance level of the entire data for this flight was calibrated against the observed spectral data of this emission. Overall, eight interferogram data were used to extract the blackbody calibration spectra. As noticed in Figure 1, there is a considerable difference between the temperature measurements made at the two locations on the flight package, one at the blackbody source and another under the crushpad. The temperature value of 263°K seemed quite different from the temperature of the balloon environment, which was in a range of 230° to 240° K at the altitude of 95 K ft. The raw spectral data observed for the blackbody emission was averaged over eight data and further smoothed. The obtained spectrum is shown in Figure 2. The spectral response of the instrument was determined by comparing the obtained curve and the blackbody radiance calculated at 263 K by

$$B(\sigma) = 2hc^2\sigma^3 \frac{1}{e^{\frac{hc\sigma}{kT}} - 1} \cdot$$

$$= 1.1909 \times 10^{-12} \frac{\sigma^3}{e^{\frac{1.4388\sigma}{T}} - 1} \text{ W/ cm}^2\text{/ steread/ cm}^{-1}.$$

Figure . Spectrometer's response with respect to the blackbody calibration source at 363 F

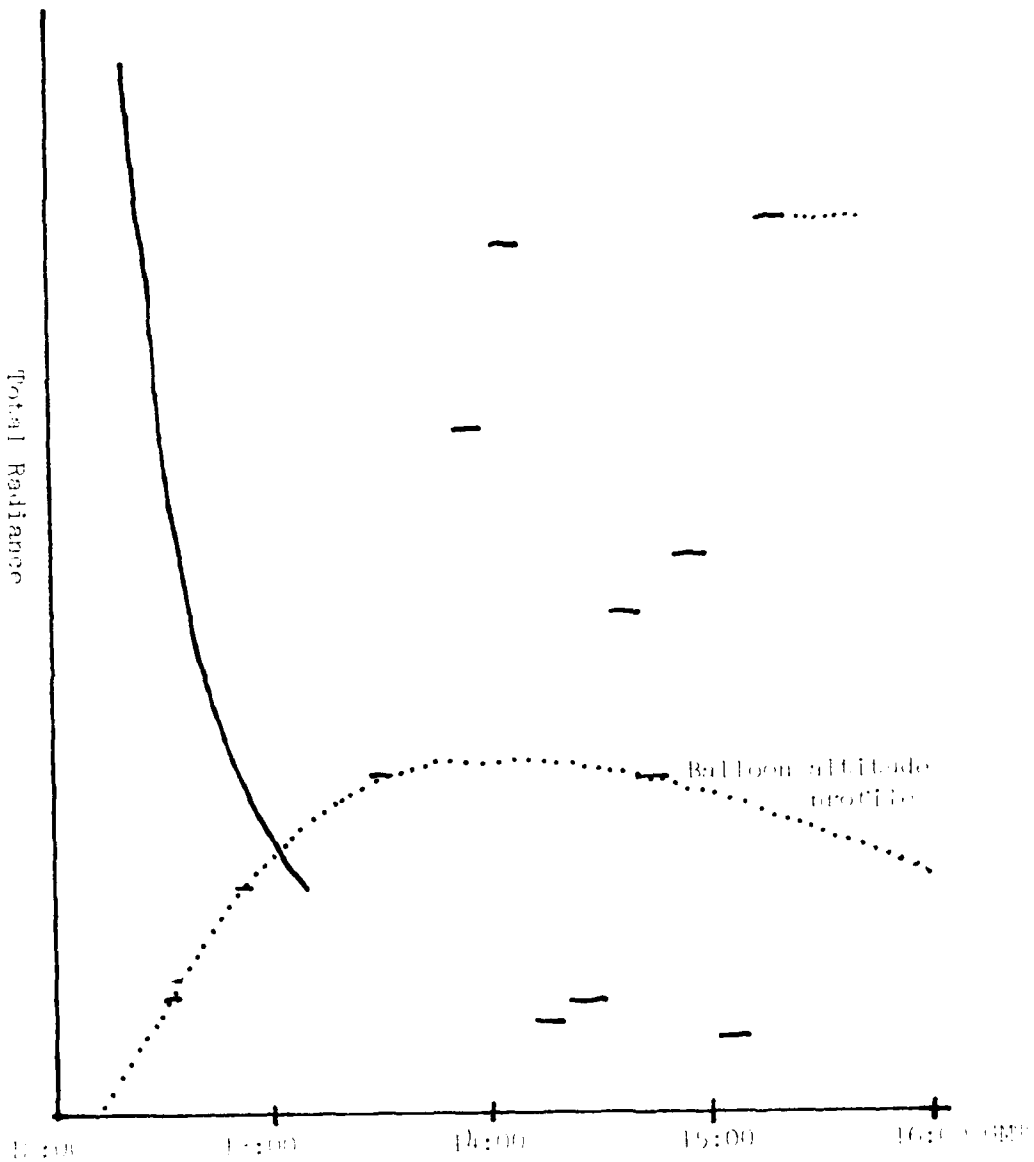

Figure 4. Ground observed total radiance level as a function of GMT. The dotted curve is for the balloon altitude.

where σ is the wavenumber in cm^{-1}. The total radiance level received for each interferogram observation is presented in Figure 4. The data are directly extracted from the central maximum value in the observed interferogram data.

Spectral Data

The obtained data may be classified into six major categories indicated below, in accordance with the elevation angle of the interferometer field of view with respect to the horizon.

I 7.5°

II 1.7°

III -0.4° tangent height = 29 km

IV -2.9° tangent height = 21 km

V -5.4° tangent height = 0.5 Km

VI -90°

As seen in the spectrometer response curve shown in Figure 3, the spectral observation has a cut-off at approximately 575 cm^{-1}. At the time of writing this report, the spectral data processed from the recorded interferogram data are those indicated in Figure 1. Table I lists those processed.

The balloon was launched, with the elevation angle set at

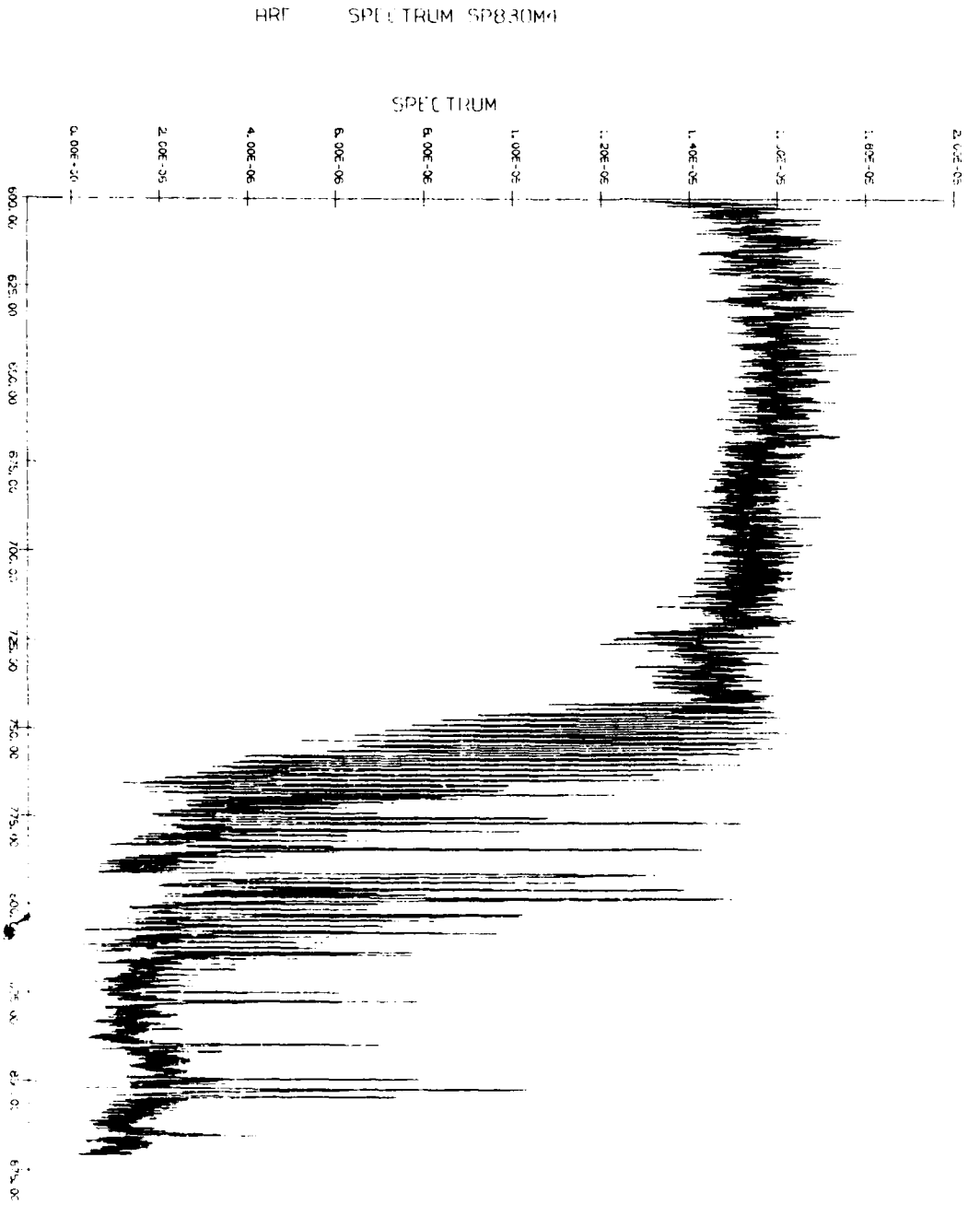

Figure 5. Spectrum observed with an elevation angle of [illegible] and azimuth of [illegible].

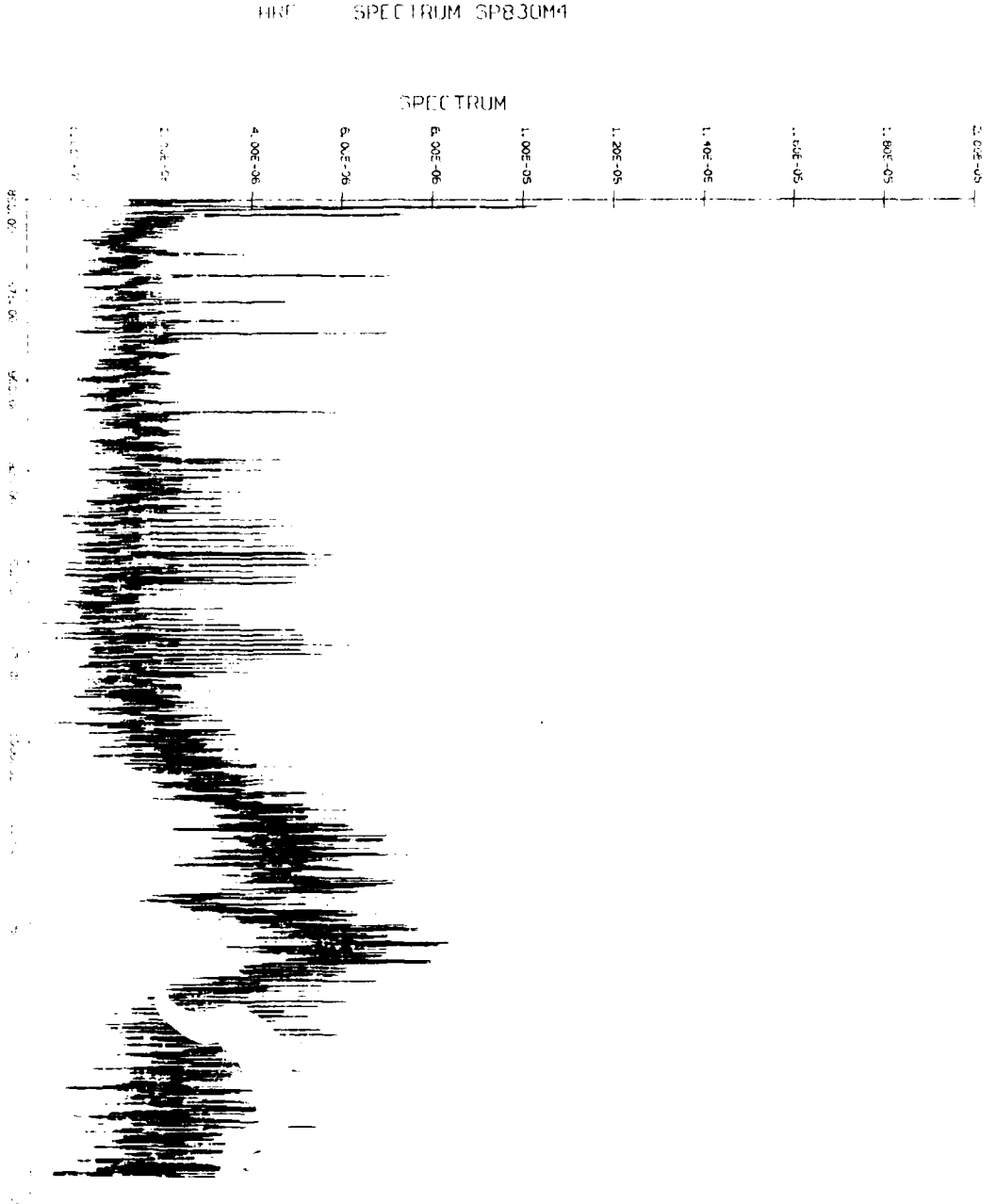

[illegible] spectrum recorded with an elevation angle of 7.5 degrees [illegible] resolution of 4 cm^{-1}; 250-1100 cm^{-1}.

HRR SPECTRUM SP830E5

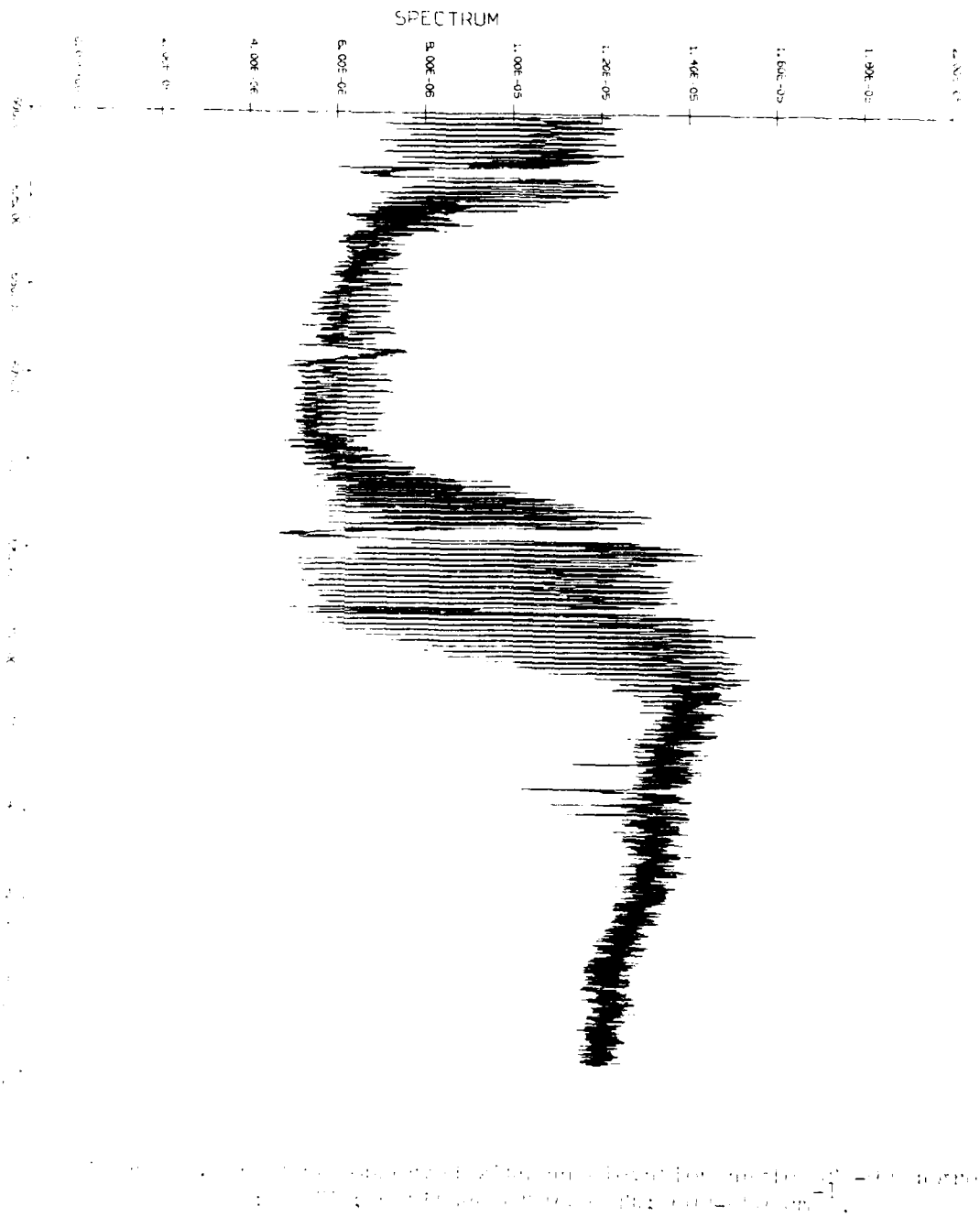

are more easily recognizable in emission than absortion. In contrast to the HNO case, the species which do not form a thin layer, exhibit a quite different picture. For those molecules which make distribution either uniformely in the atmosphere or in a thick layer, the absorption lines of relatively weak strength are clearly identified in the -5.4-degree data.. The H O lines with high J' in the pure rotation band and the band, the CO lines in the 00011-10001 and the 00011-10002 band, and the N O lines are clearly visible.

The data shown in Figures 16 and 17 were taken in the down-looking mode. The O and CO features are the principal absorption observable in this mode. The lines of CO 15 micron band clearly show emission characteristic, indicating that the stratospherice temperature is indeed higher than the tropopause temperature. In these down-looking spectra, some H O absorption lines are observable, although they are not many. The radiative temperature of the background is 295 degrees , higher than the background observed at an elevation angle of -5.4 degrees.

The spectral features associated with specific molecules and/or specific spectral region are found observable in specific sight conditions. For example, the HNO feature is best observable in the -2.9-degree data. Figure shows a detail of

HRF SPECTRUM SP83047

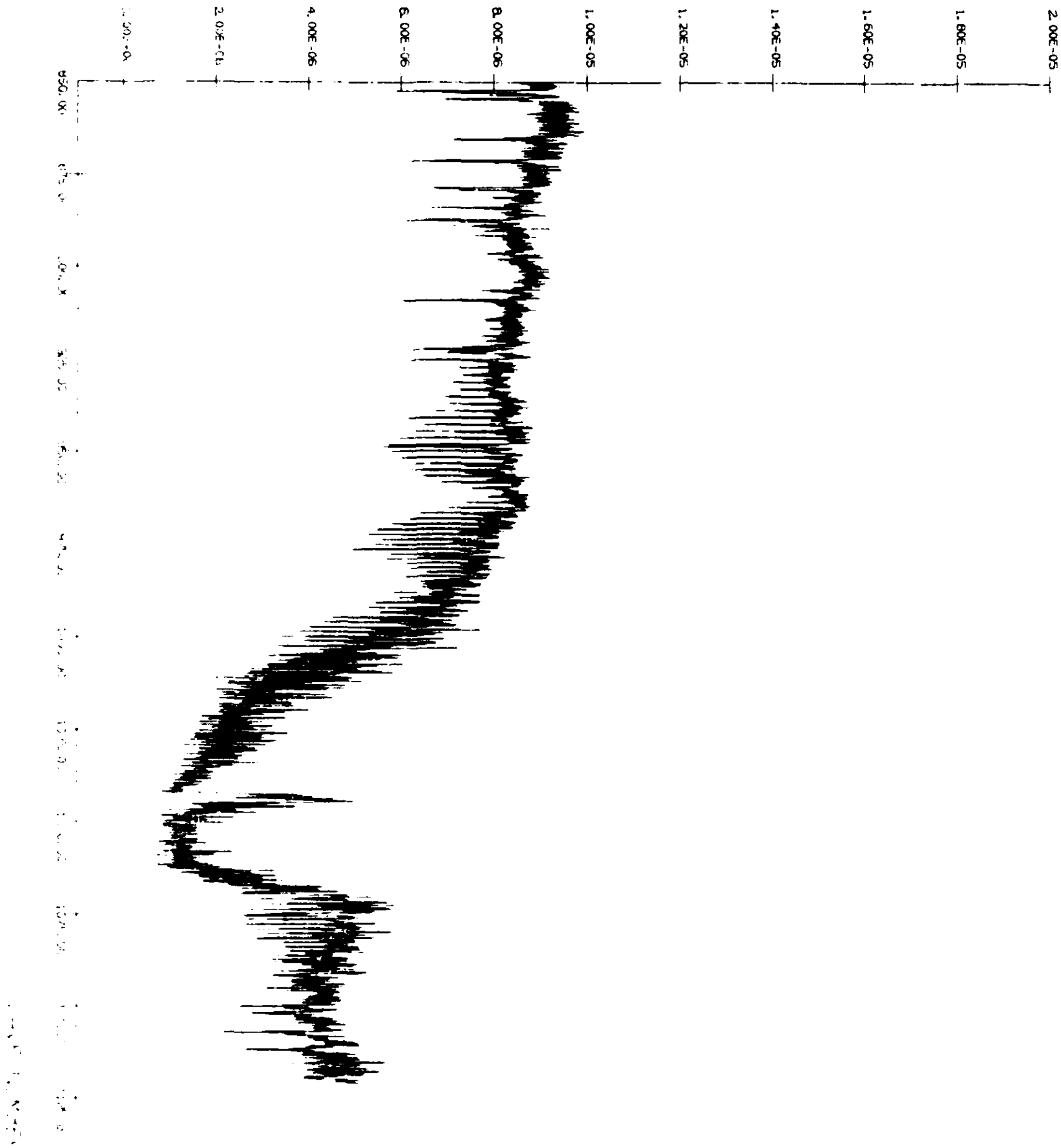

[illegible] with an elevation angle of –[illegible] degrees. [illegible] 850–1100 cm^{-1}.

ARF SPECTRUM SP83047
SPECTRUM
0.00E+00
2.00E-06
4.00E-06
6.00E-06
8.00E-06
1.00E-05
1.20E-05
1.40E-05
1.60E-05
1.80E-05
2.00E-05
600.00
625.00
650.00
675.00
700.00
725.00
750.00
775.00
800.00
825.00
850.00
875.00

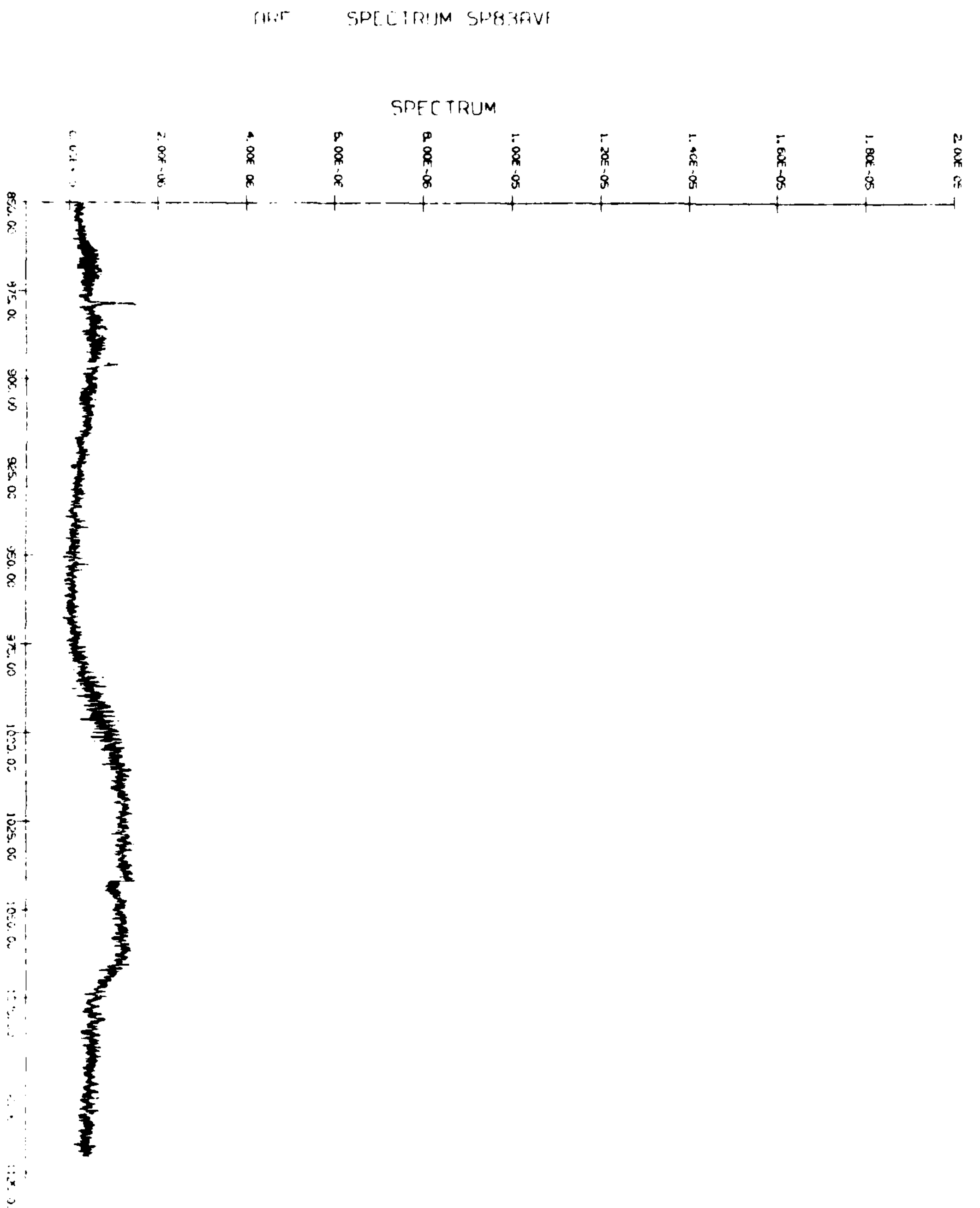

Figure [illegible]. Spectrum observed with an elevation angle of −[illegible] degrees. Data averaged over [illegible] spectra [illegible]–1[illegible]:30 GMT; altitude [illegible]; [illegible] cm^{-1}

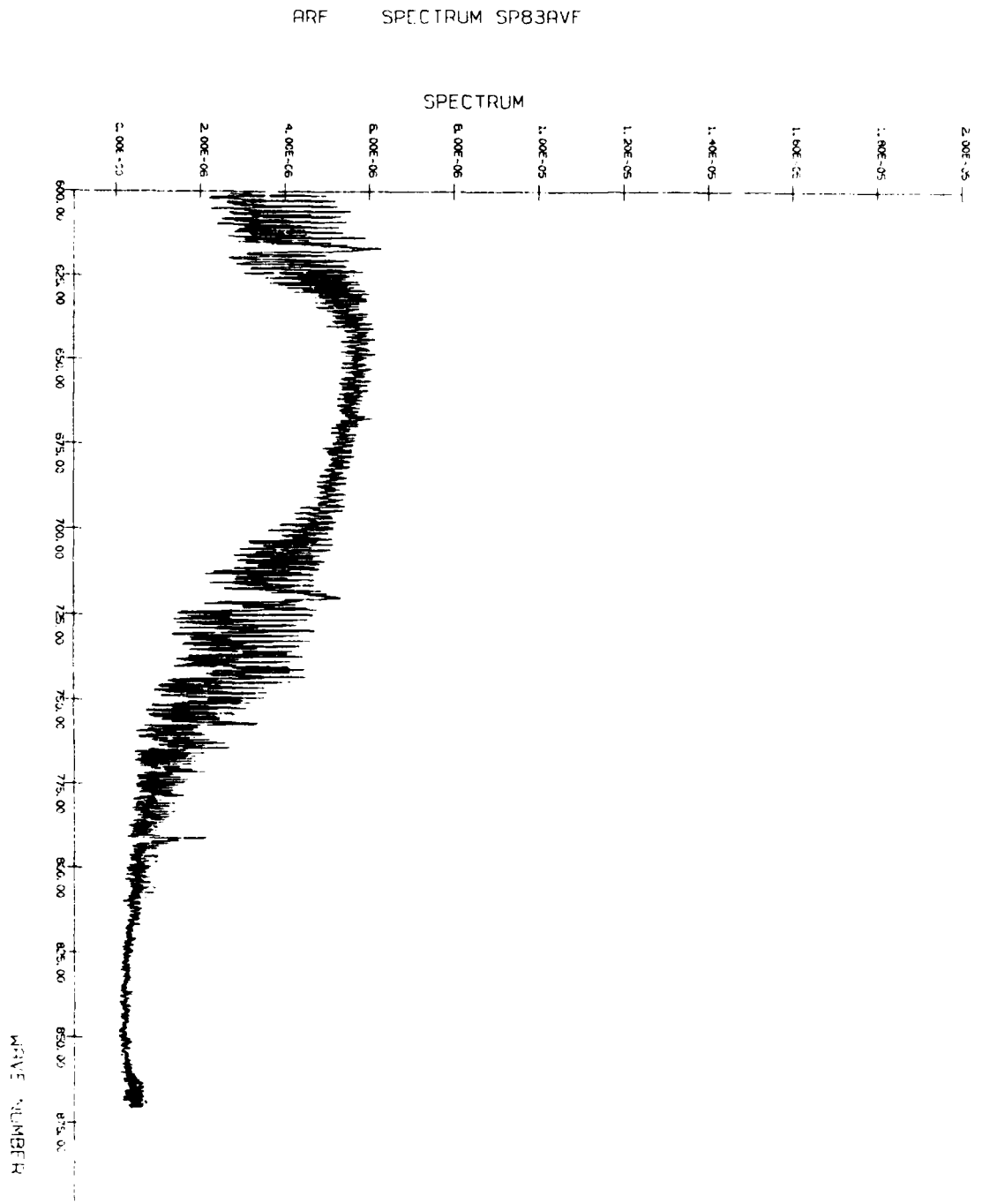

Figure 12. Spectrum observed with an elevation angle of -2.0 degrees. Data averaged over 6 spectra [illegible], 500–850 cm^{-1}.

the elevation angle set at 7.5 degrees. The observable feature is due to CO_2 only. The disappearance of the O_3 feature indicates that the major concentration of this molecule occupies the atmosphere below 30 Km.

The spectral data taken with an elevation angle of -2.9 degrees are shown in Figures 12 and 13. The features observable in the 880 cm-1 region are identified as the ν_5 and $2\nu_9$ bands of HNO_3. Inspecting together with other data, we find that the HNO_3 feature is seen best with the elevation angle of -2.9 degrees. The tangent height for this line of sight is approximately 20 Km. The data indicate that the HNO_3 molecules in the atmosphere reach maximum abundance around the tropopause.

The spectral data taken with an elevation angle of -5.4 degrees are shown in Figures 14 and 15. Most of the atmospheric lines are observable as the absorption lines against the radiative background of approximately 275 K. The emission feature is seen in the CO_2 ν_2 band region, indicating that the temperature in the vicinity of the balloon is at a slightly higher temperature than the background. The HNO_3 features observable in the -2.9 degree data are hardly recognizable for this line of sight. We may conclude that the minor atmospheric species,in particular those formed in a thin layered structure,

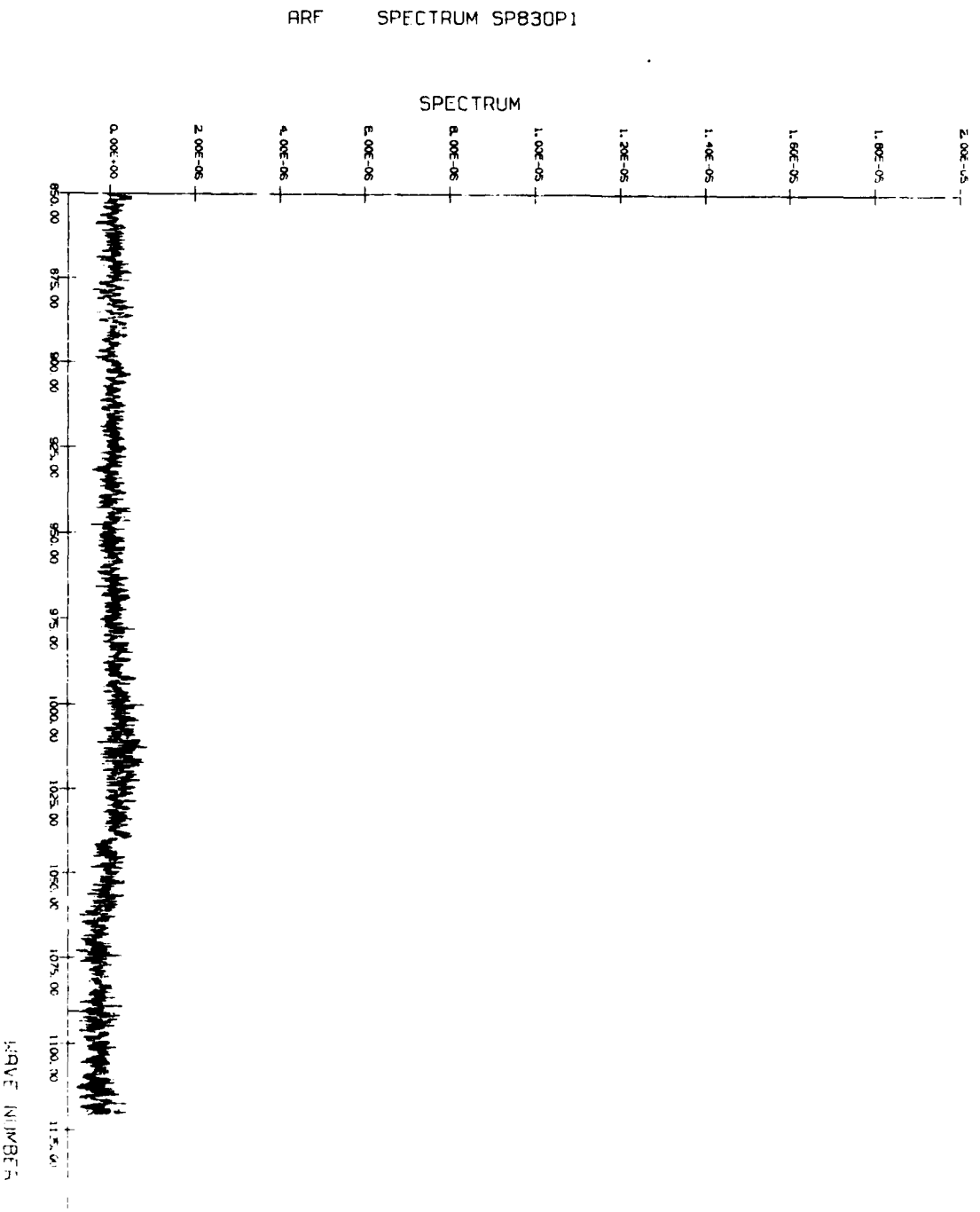

Figure 11. Spectrum observed with an elevation angle of 1.5 degrees. 15:06 GMT; altitude 95.5 Kft; 850–1100 cm^{-1}.

HRF SPECTRUM SP830P1

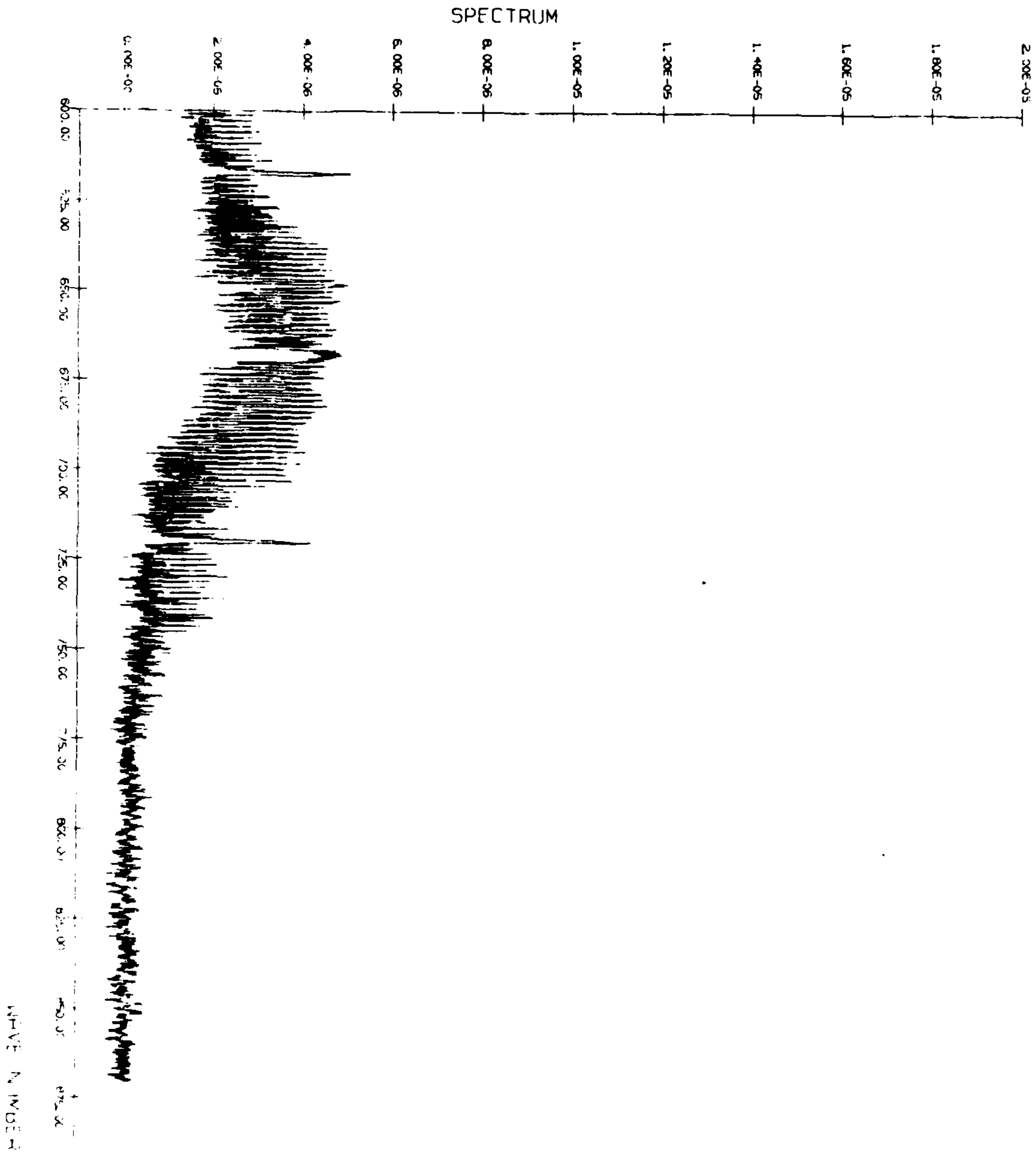

Figure 10. Spectrum observed with an elevation angle of 7.5 degrees. [illegible] GMT; altitude 95 K ft; 600–850 cm^{-1}.

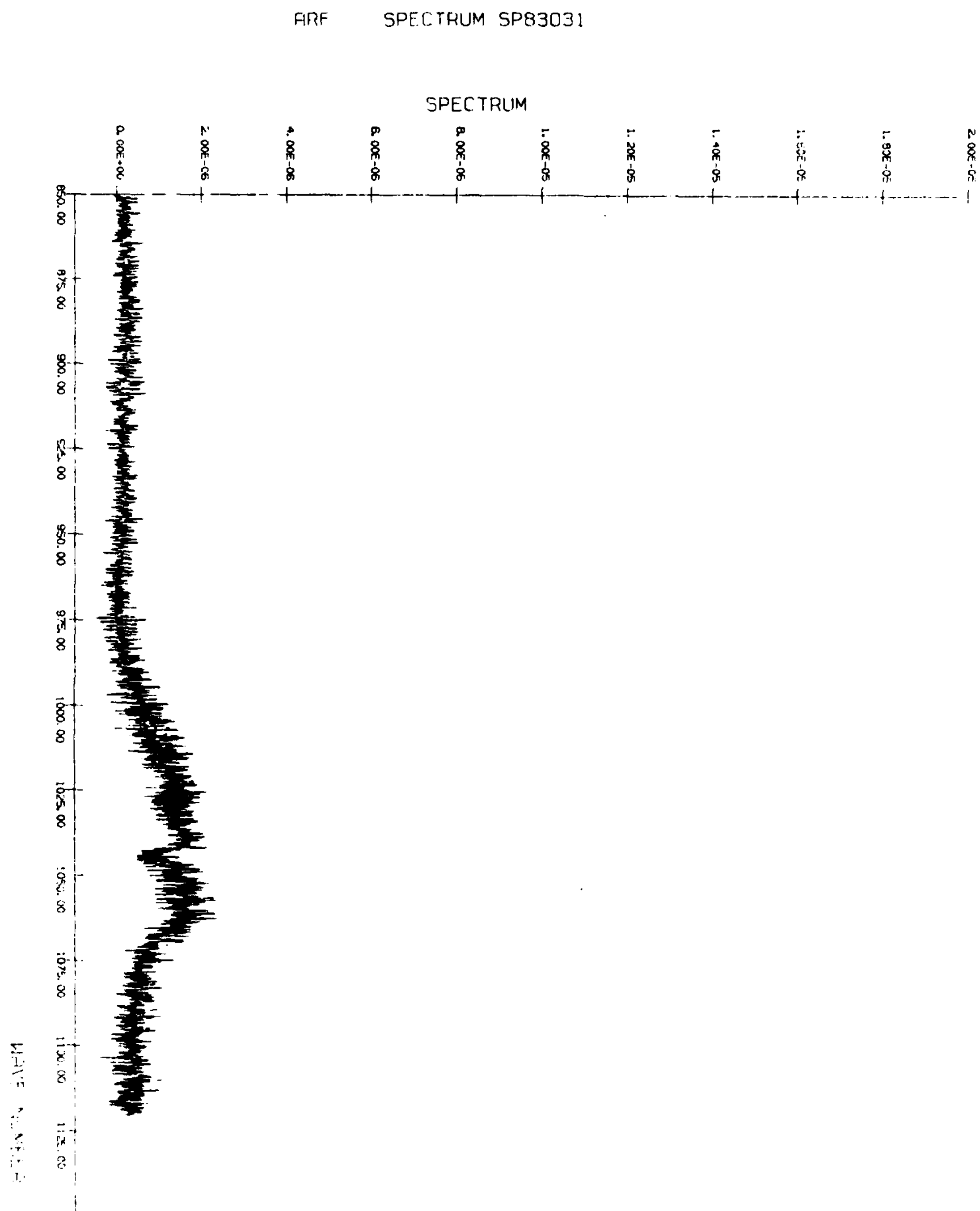

Figure 9. Spectrum observed with an elevation angle of -0.[illegible] degrees. [illegible] CST; altitude of [illegible] m; 850-1100 cm^{-1}.

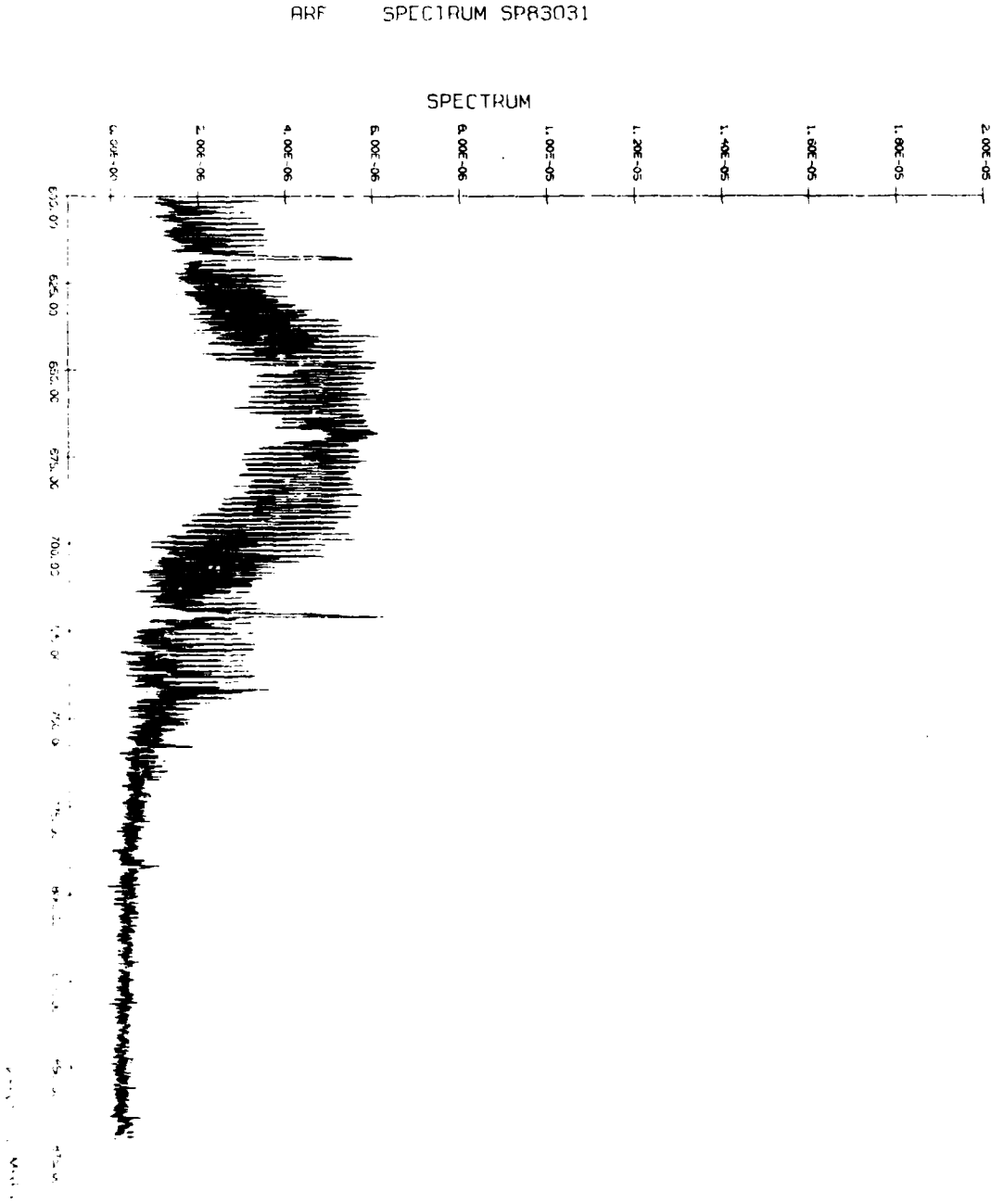

Figure . Spectrum observed with an elevation angle of -0.1 degrees

7.5 degrees. The observation with this elevation angle continued until the balloon reached the altitude of 80 K ft. Unfortunately the PCM signal became not-processable after the balloon reached 50 K ft [7 PCM tape],and remained so until the down-looking mode. The total radiance level varied approximately by a factor of 10 as the balloon ascended from ground level to the ceiling altitude of 95K ft. Figures 4 through 7 show two typical spectra observed at relatively low altitude with an elevation angle of 7.5. The Q branch of the $CO_{2}\nu_{2}$ band at the 670 cm-1 region exhibits a radiance temperature approximately 10 degrees higher than the rest of the spectral region nearby. The opacity of this Q branch region is extremely high. The Q branch radiance value of this $CO_{2}\nu_{2}$ band serves as a thermometer of the immediate vicinity of the instrument. Thus it may be interpreted that the high radiative temperature shown by this Q branch emission is due to a warm air mass carried by the balloon package in its proximity.

The spectral data taken with -0.4 degree elevation angle are shown in Figures 8 and 9. The data were taken at the ceiling altitude. The O_{3} feature is clearly observable in the data , while no $H_{2}O$ lines are present.

The spectral data shown in Figure 10 and 11 were taken with

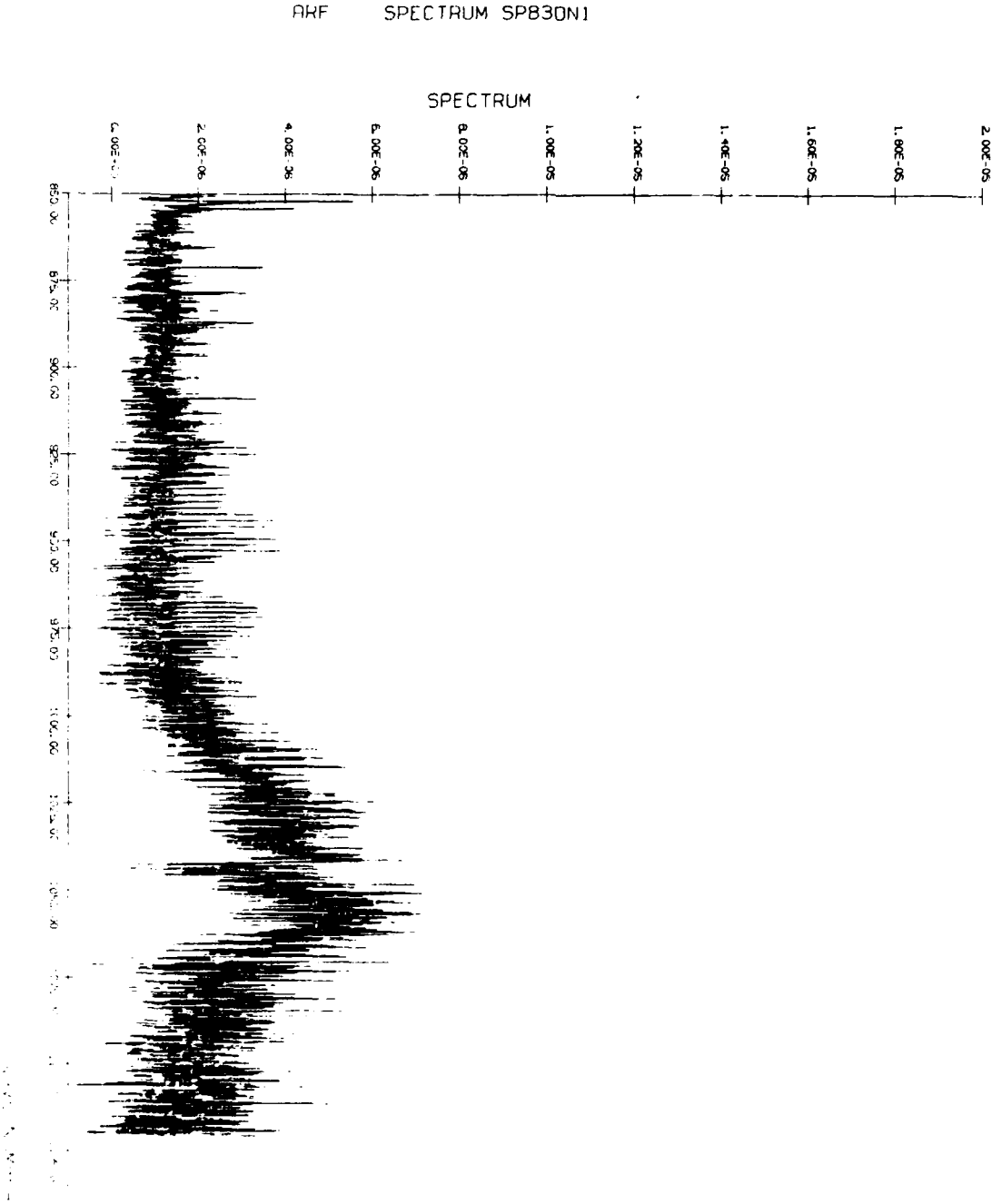

. Spectrum observed with an elevation angle of 7.5 degrees.
; altitude = 5 Mm; 830-1100 cm^{-1}.

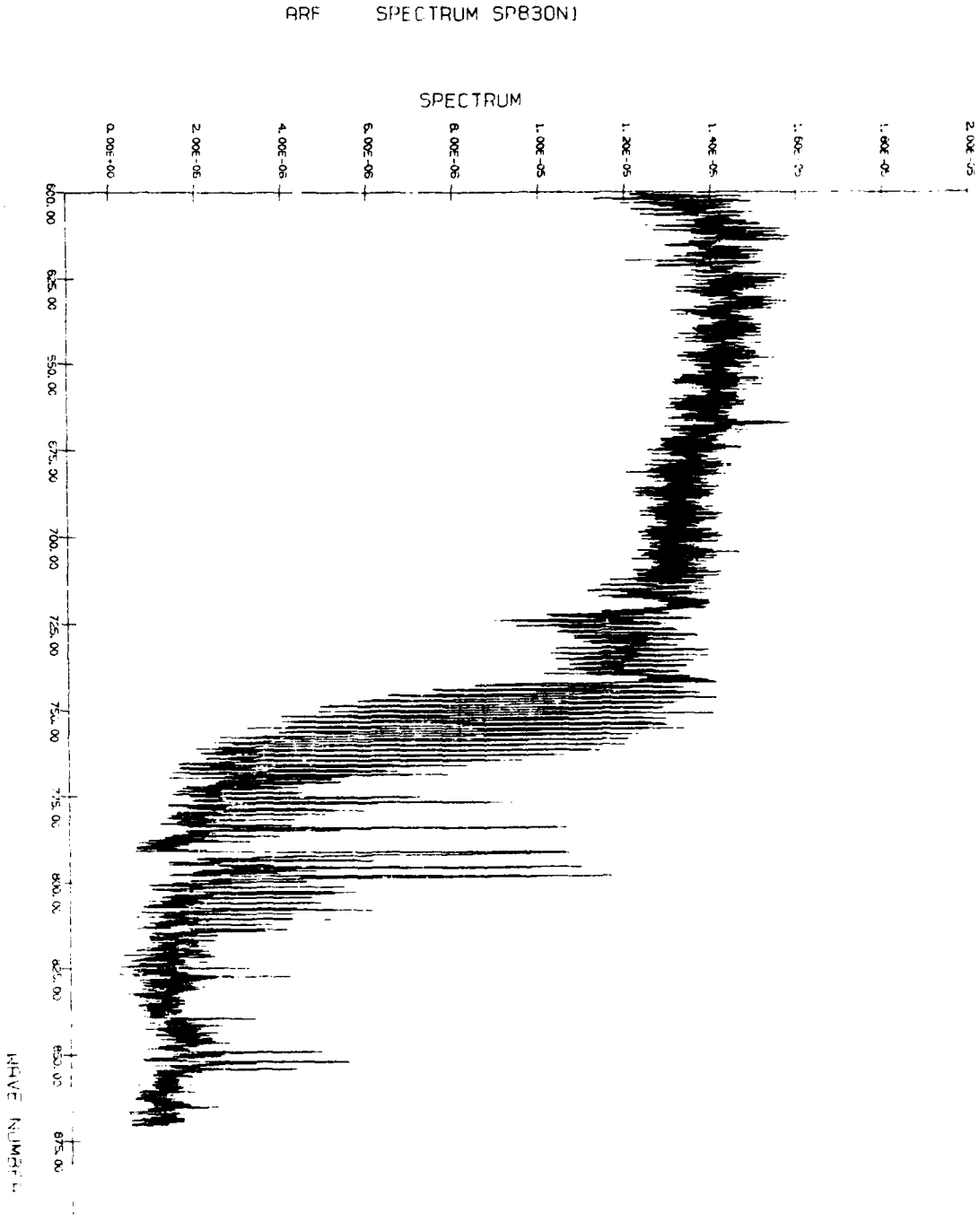
ARF SPECTRUM SP830N1
SPECTRUM
0.00E+00
2.00E-06
4.00E-06
6.00E-06
8.00E-06
1.00E-05
1.20E-05
1.40E-05
1.60E-05
1.80E-05
2.00E-05
600.00
625.00
650.00
675.00
700.00
725.00
750.00
775.00
800.00
825.00
850.00
875.00
WAVE NUMBER

PRF SPECTRUM SP830B5

SPECTRUM SP83AVI

SPECTRUM

the HNO_3 spectrum. Table II lists the observed peak of these emission lines. The extremely complex structure in the 600-750 cm^{-1} region is best obsevable in the 7.5-degree data . Figures 19 and 20 show this spectral region in detail. Relatively weak H_2O lines were best observed in the -5.4-degree data, as shown in Figure 21. Table III provides the wavenumber position of the observed H_2O lines. The ozone band at the 1000 cm^{-1} region is shown in Figure 22 for its absorptive feature and Figure 23 for its emissive feature. The N_2O feature in the 1120-1200 cm^{-1} is detailed in Figure 24. The data are noisy because of the low spectral response exhibited by the spectrometer.

The spectral data presented in this report are those typical ones obtained in this flight. A digital 9-track magnetic tape, which contains 47 spectral data taken at various phase of this experiment, is attached as a supplement to this report.

In addition several plots of some spectral data are attached for demonstrating the spectral resolution and the signal-to-noise ratio of the obtained data.

The observed emission data with an elevation angle of -0.4 degrees are compared with the theoretical data computed using the

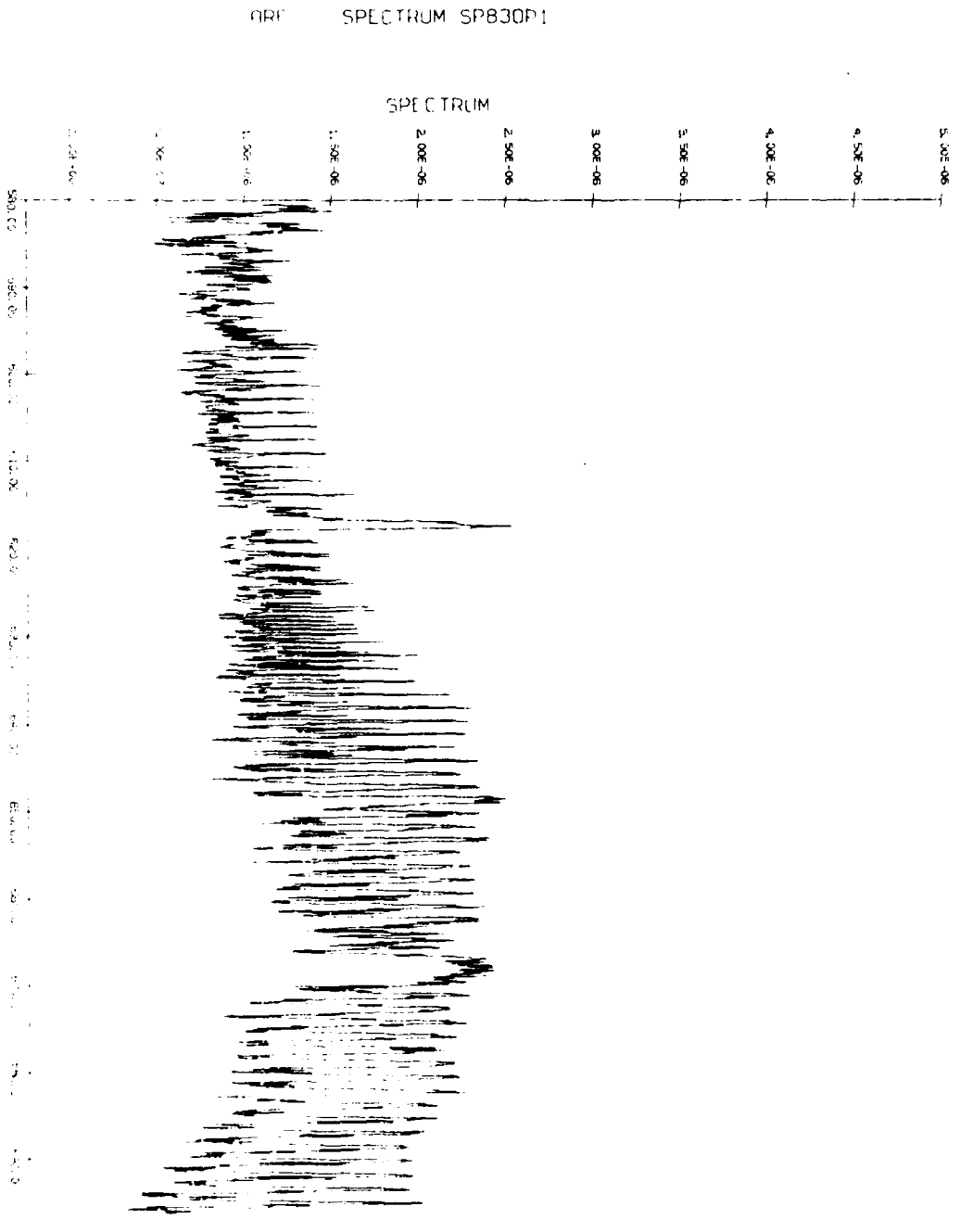
ORF SPECTRUM SP830P1
SPECTRUM
1.50E-06
2.00E-06
2.50E-06
3.00E-06
3.50E-06
4.00E-06
4.50E-06
5.00E-06

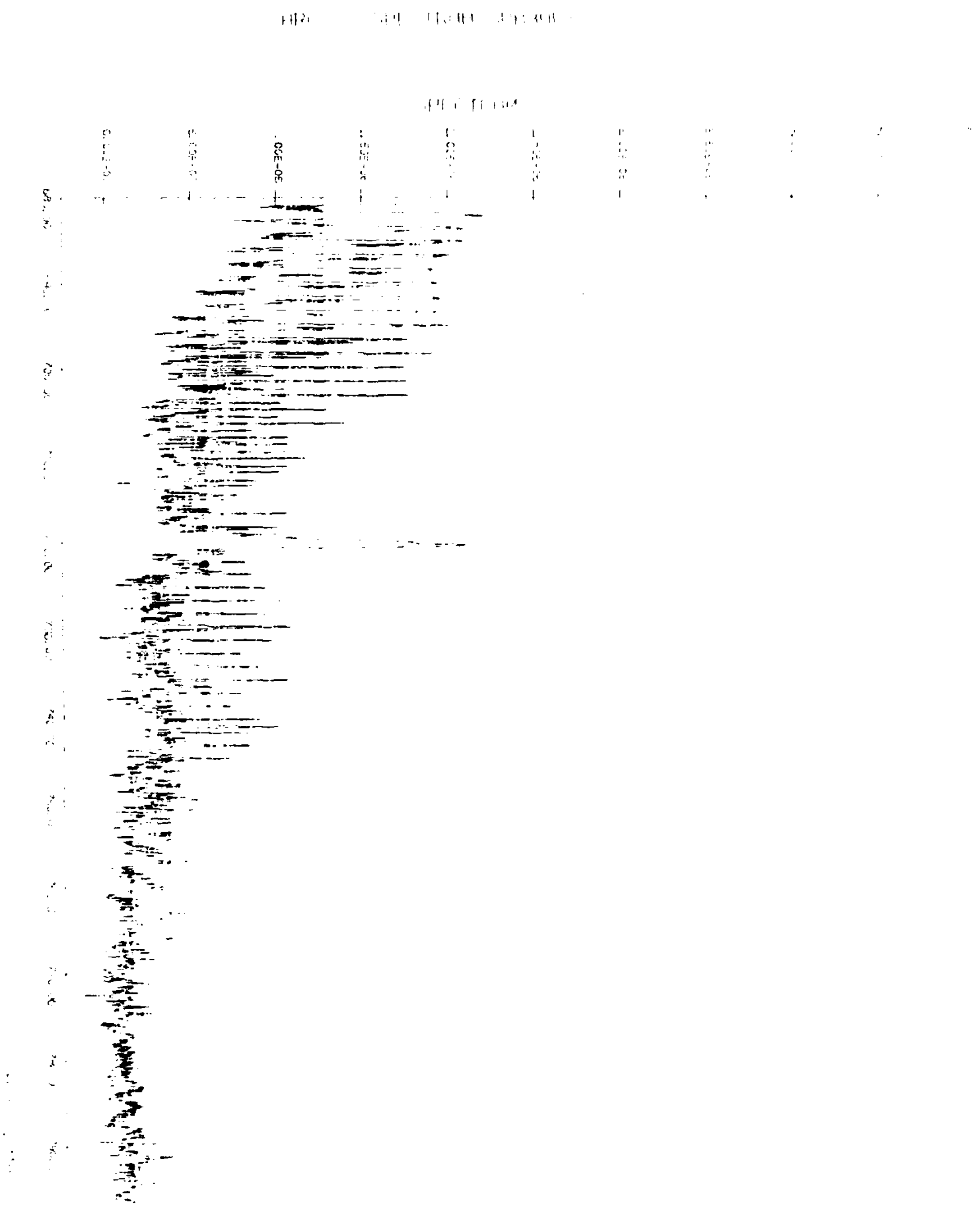

Figure [illegible]. Observed spectrum in [illegible] – [illegible] cm^{-1} [illegible].
Elevation angle [illegible] degrees [illegible].

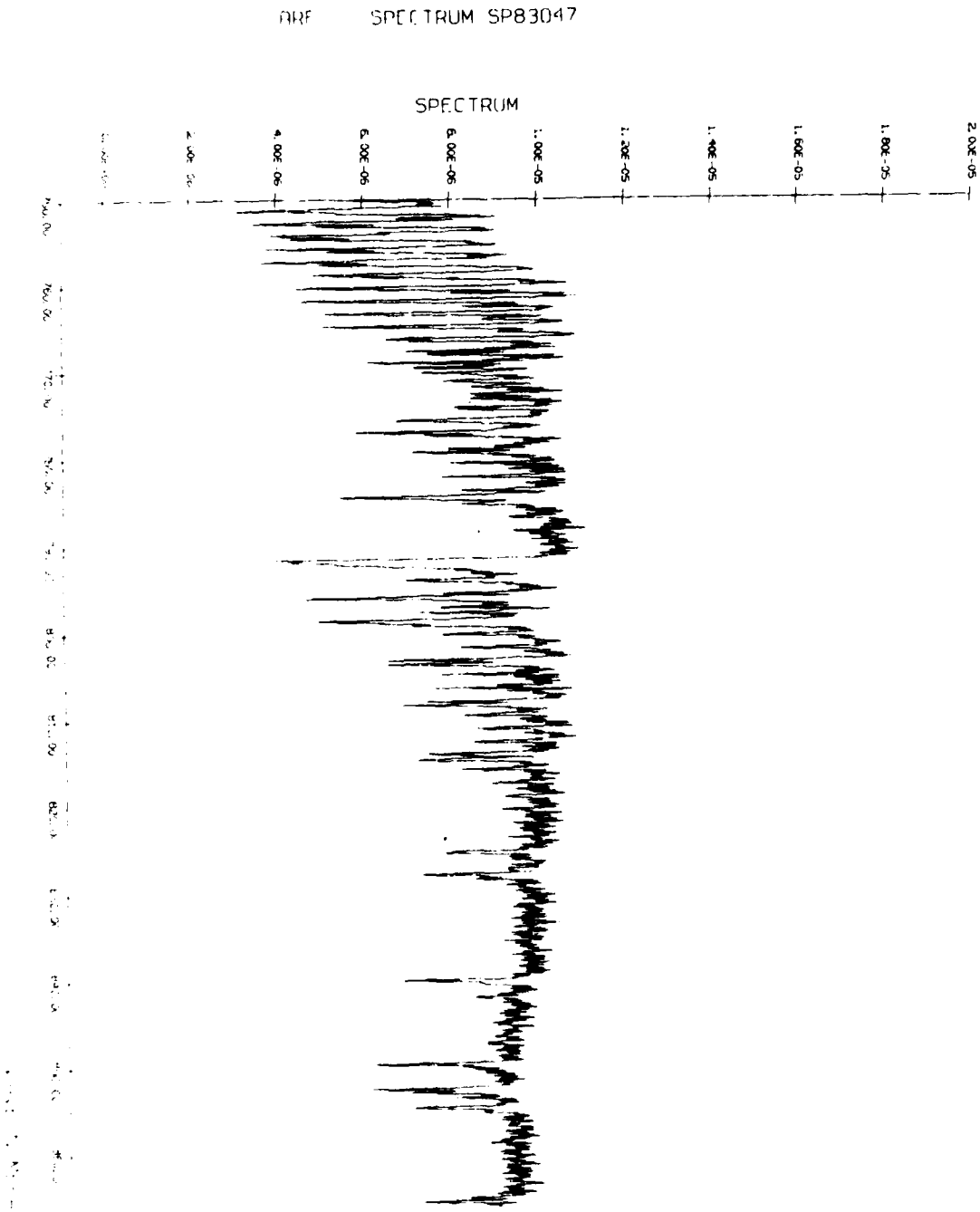
ARF SPECTRUM SP83047
SPECTRUM
4.00E-06
5.00E-06
6.00E-06
1.00E-05
1.20E-05
1.40E-05
1.60E-05
1.80E-05
2.00E-05

Figure 1(b). Observed spectrum for the 950– 850 cm^{-1} region.
[illegible] for angle = 1.3 degrees off Bragg [illegible].

SPECTRUM SP83047
SPECTRUM
2.00E-05

SPECTRUM SP83047
SPECTRUM

SPECTRUM SP83031

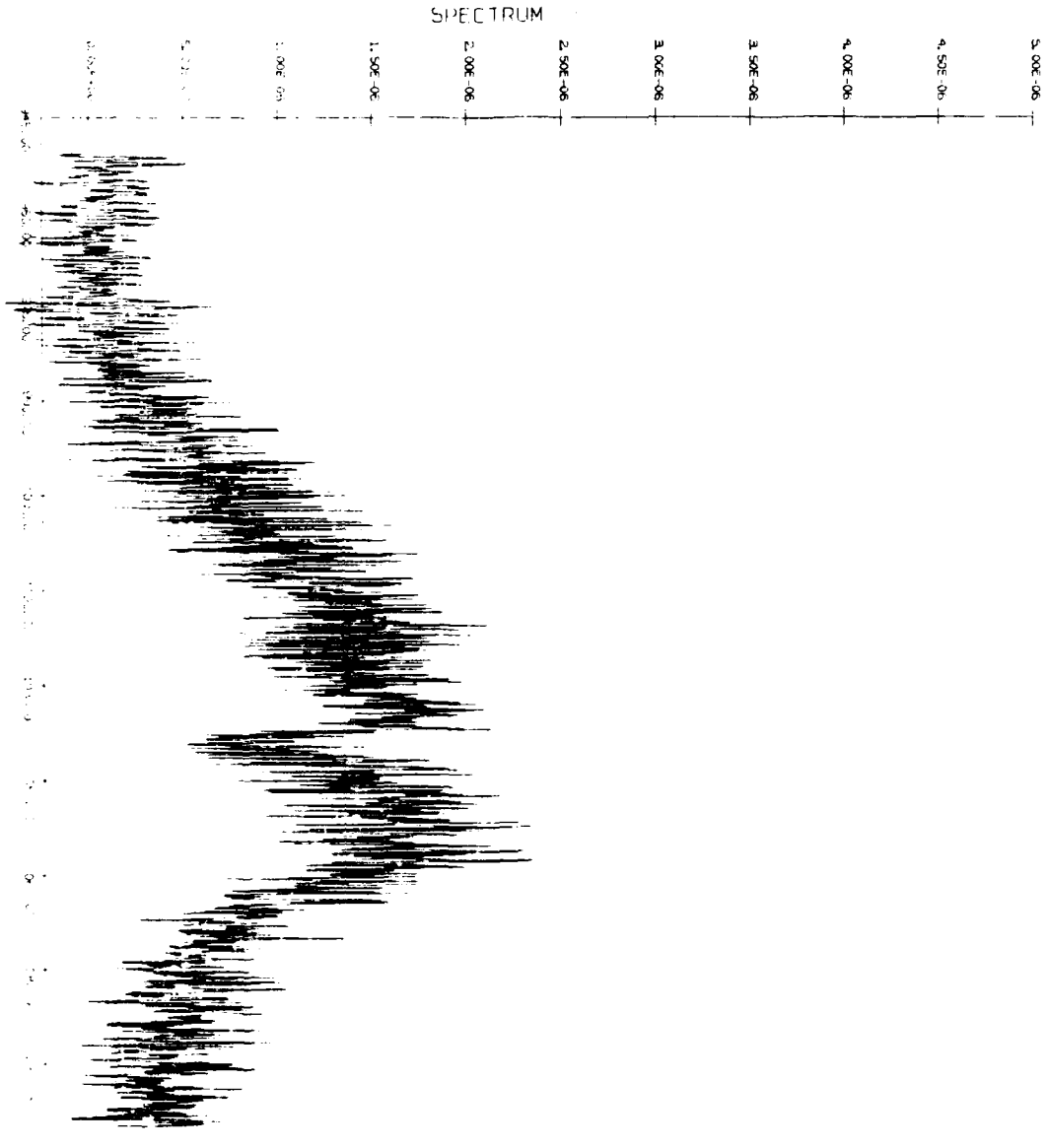

ARF SPECTRUM SP83047

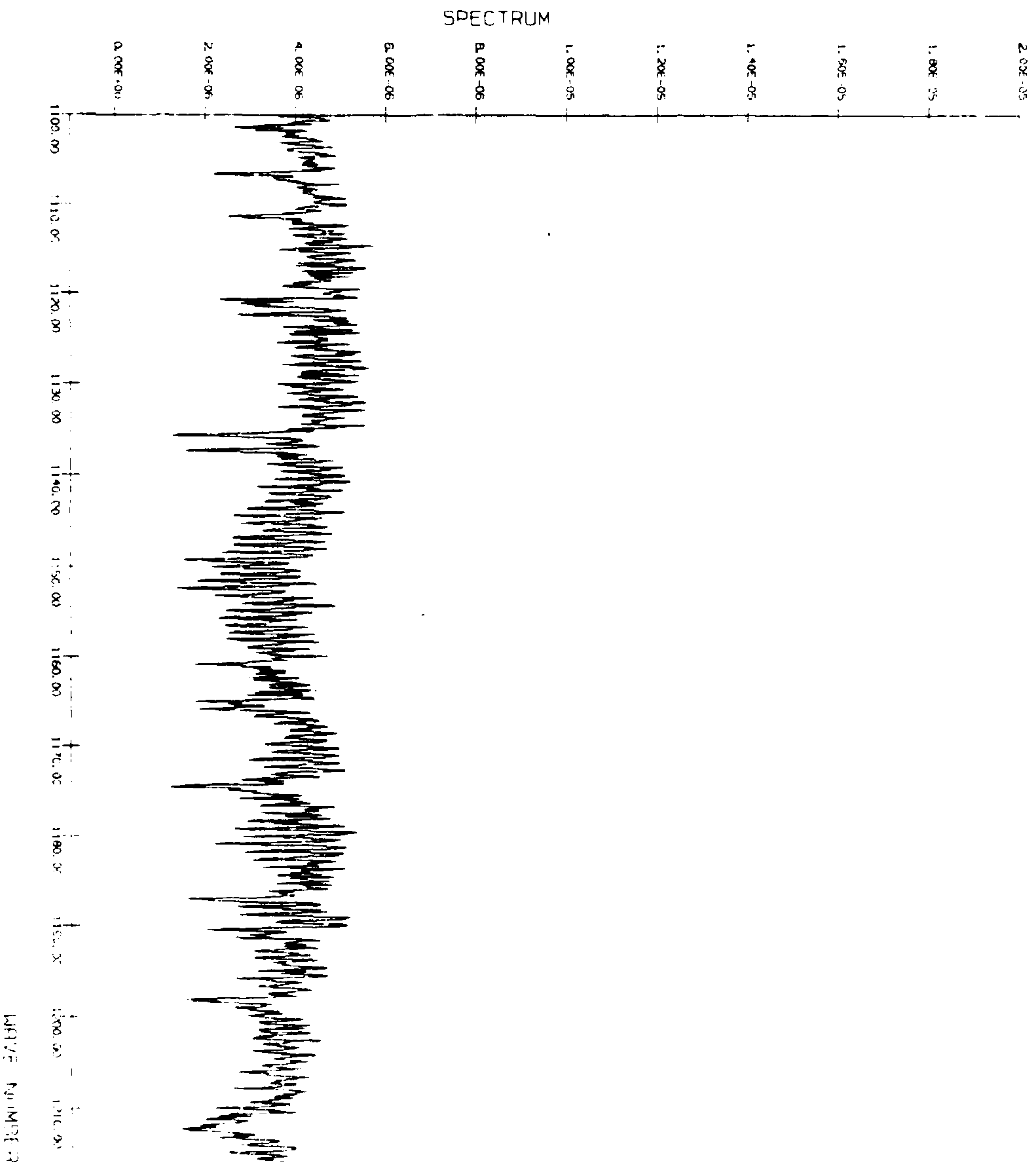

AFGL atmospheric line compilation data in Figures 25 through 30. The lines in the synthetic spectrum are computed for the CO_2 column density of 8.1×10^{21} /cm^2 with a pressure of 0.14 atmospheric pressure and a temperature of 230 K.

The data taken with an elevation angle of -2.9 degrees are compared with the theoretical data in Figures 31 through 36. The synthetic spectrum is generated for the CO_2 column density of 5.8×10^{22} /cm^2 at 0.14 atmospheric pressure and 230 K.

In these sets, the synthetic data show that their line widths slightly broader than the observed, probably because of the higher pressure assumed in the computation. Nonetheless, these figures, the observed and the theoretical widths, should be close enough for the comparison purpose. The synthetic data prior to application of the instrument function smearing show that the lines are very narrow compared with the instrument function full width of 0.12 cm^{-1} at the half height. Thus the data provide a good refernce for the spectral resolution figure of the observed lines for the horizontal line of sight at the balloon ceiling altitude of approximately 29 km.

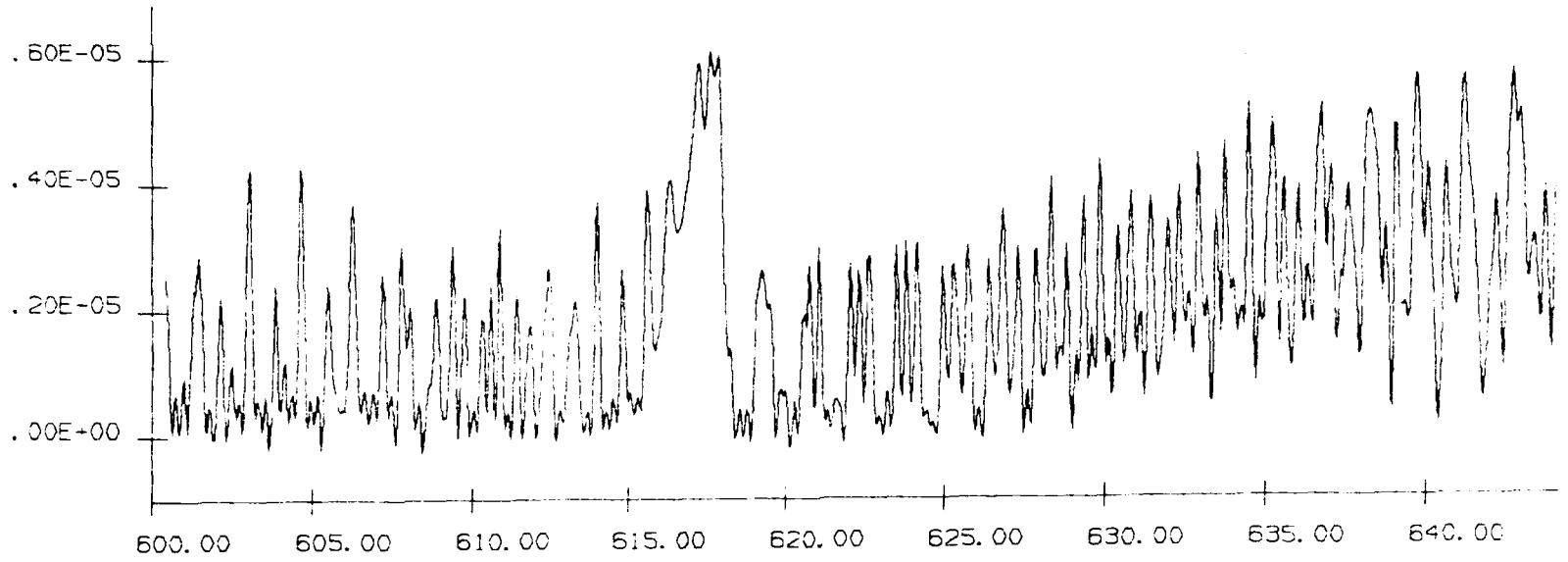
.60E-05
.40E-05
.20E-05
.00E+00
600.00
605.00
610.00
515.00
620.00
625.00
630.00
635.00
640.00

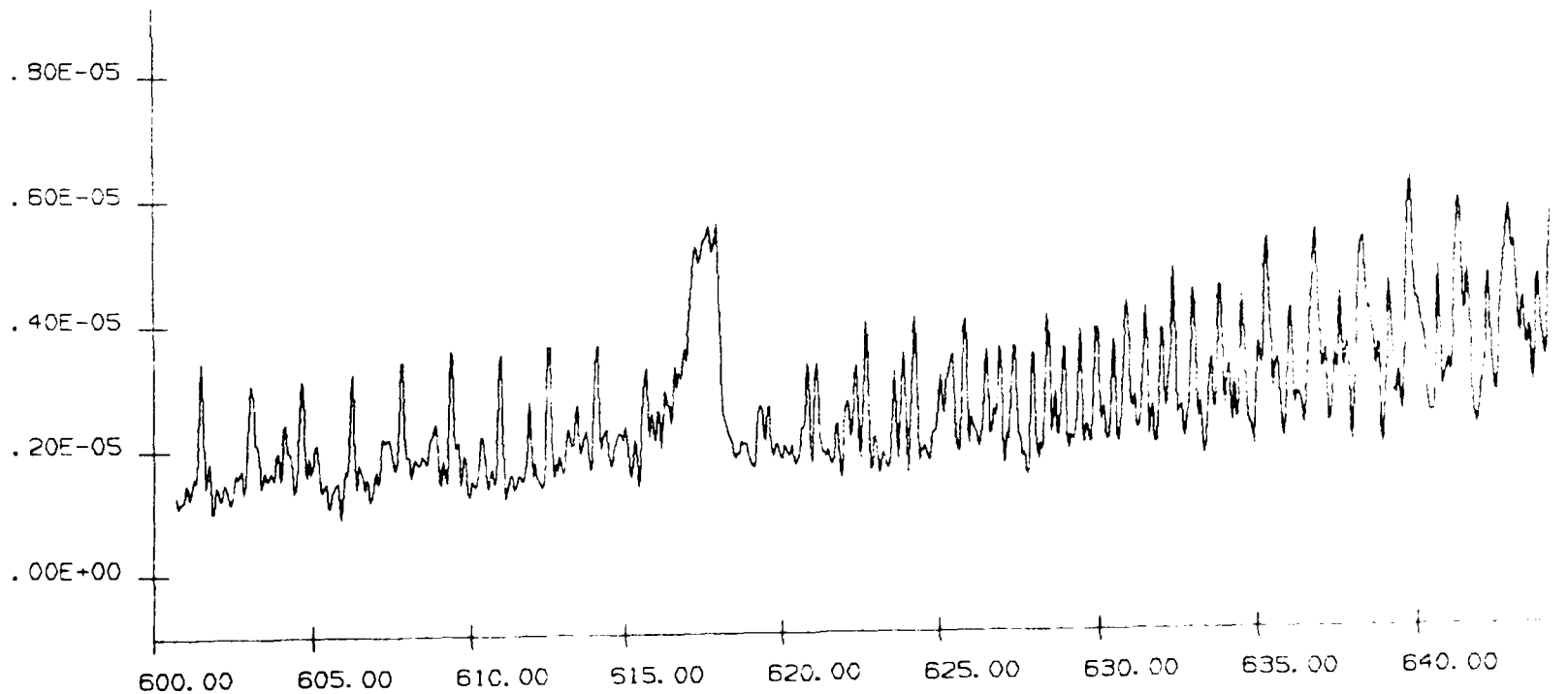
.80E-05
.60E-05
.40E-05
.20E-05
.00E+00
600.00
605.00
610.00
515.00
620.00
625.00
630.00
635.00
640.00

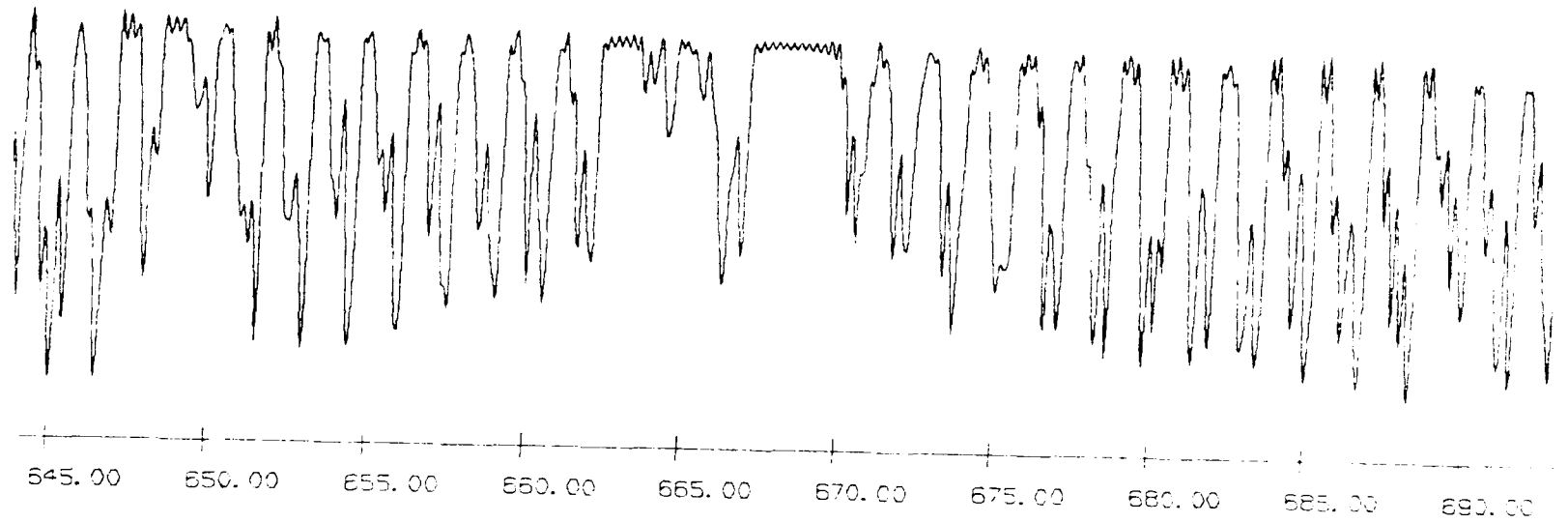
645.00
650.00
655.00
660.00
665.00
670.00
675.00
680.00
685.00
690.00

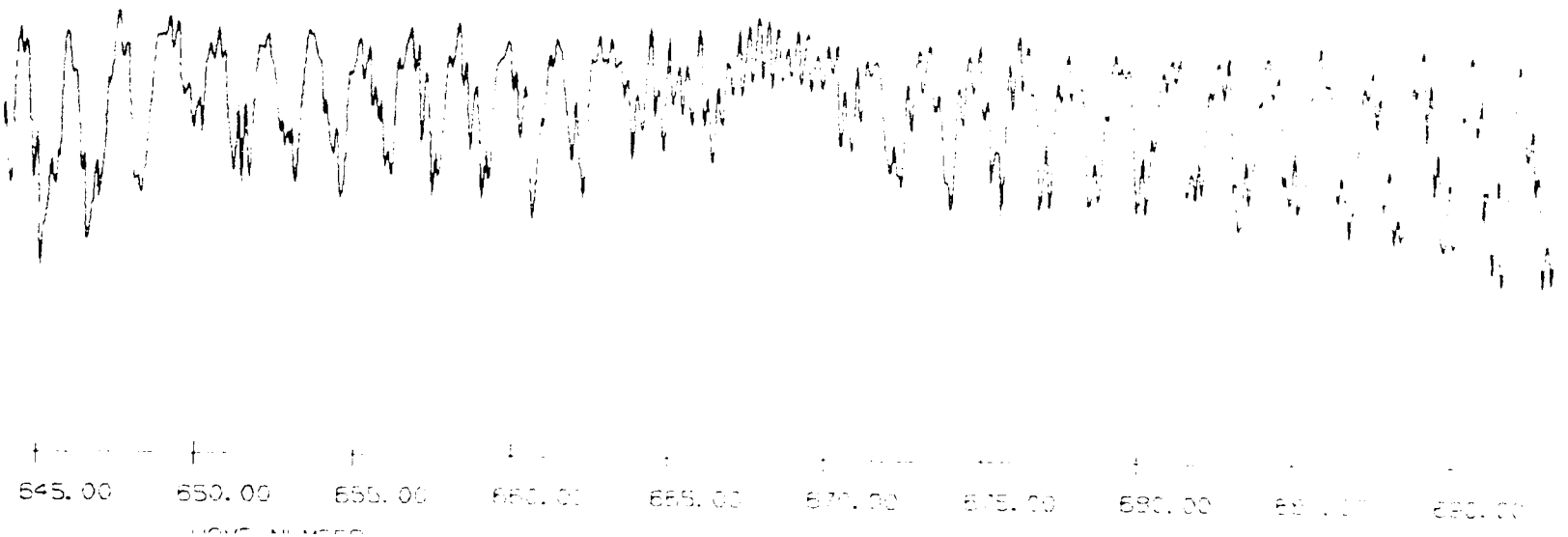
645.00
650.00
655.00
665.00
670.00
675.00
680.00

Table III

Observed position of the H_2O lines

776.6
780.1
784.0
795.6
802.7
803.1
807.9
814.1
824.8
827.3
839.5
841.5
849.2
852.0
852.5
854.2
864.6
865.0
870.8
878.1
880.6
883.4
886.8
888.2
890.9
905.8
908.5
921.7
922.7
924.6

Table II

Observed line position of the HNO_3 lines

862.26	884.98
862.68	885.40
863.29	885.76
863.65	886.25
864.55	886.61
864.97	887.39
865.88	888.17
866.30	888.54
886.78	888.96
867.26	889.32
867.68	889.74
868.11	890.10
868.59	890.46
869.01	890.83
869.43	891.61
869.91	892.39
870.34	903.48
870.76	903.84
871.24	905.35
871.66	905.71
872.08	
872.93	
878.35	
878.59	
879.74	
882.57	
882.99	

Table 1 Data Processed

Code	GMT	Altitude K ft	Elevation angle	View
October 23, 1983 (Day 296)				
SP830A1-A7	12:16	10	7.5	H
M1-M7	12:20	20	7.5	H
N1-N7	12:25	25	7.5	H
O1-O7	12:30	30	7.5	H
11-17	13:15	70	1.7	H
21-27	13:45	95	-	D
V1-V7	13:50	95	-	D
W1-W7	13:54	95	-	D
B1-B7	14:00	95	-	D
C1-C7	14:05	95	-	D
D1-D7	14:08	95	-	D
31-37	14:13	95	-0.4	H
E1-E7	14:17	95	-0.4	H
F1-F7	14:20	95	-0.4	H
G1-G7	14:24	95	-0.4/-2.9	H
H1-H7	14:27	95	-2.9	H
I1-I7	14:30	95	-2.9	H
J1-J7	14:33	95	-2.9/-5.4	H
K1-K7	14:37	95	-5.4	H
L1-L7	14:40	95	-5.4	H
41-47	14:45	95	-5.4	H
61-67	14:48	95	-5.4	H
71-77	14:53	95	-	B
81-87	14:55	95	-	B
91-97	15:02	95	7.5	H
P1-P7	15:06	95	7.5/-	H/D
Q1-Q7	15:10	95	-	D
R1-R7	15:15	90	-	D
S1-S7	15:18	90	-	D
T1-T7	15:22	90	-	D
U1-U7	15:25	90	-	D

References:

1 H. Sakai et al., Measurement of Atmospheric Emission Using a Balloon-Borne Cryogenic Fourier Spectrometer, Proc. International Conf. on FTIR, SPIE Publ. 386 196 (1981)

2 H. Sakai et al., Study of Atmospheric Infrared Emission Using a Balloon-Borne Cryogenic Fourier Spectrometer, SPIE Publ. 364 38 (1983)

3 H. Sakai and G. Vanasse, Atmospheric Infrared Emission Observed at Altitude of 27,000 to 28,000M. SPIE Publ. 365 165 (1983)

4 F. H. Murcray et al., Liquid Nitrogen Cooled Fourier Transform Spectrometer System For Measuring Atmospheric Emission at High Altitudes (In press)

5 H. Sakai, SCRIBE I data Analysis AFGL-TR-81-0120 (1981) AD A102262.

6 H. Sakai and G. Vanasse, SCRIBE II Data Analysis; AFGL-TR-82-0150 (1982), ADA 116 250

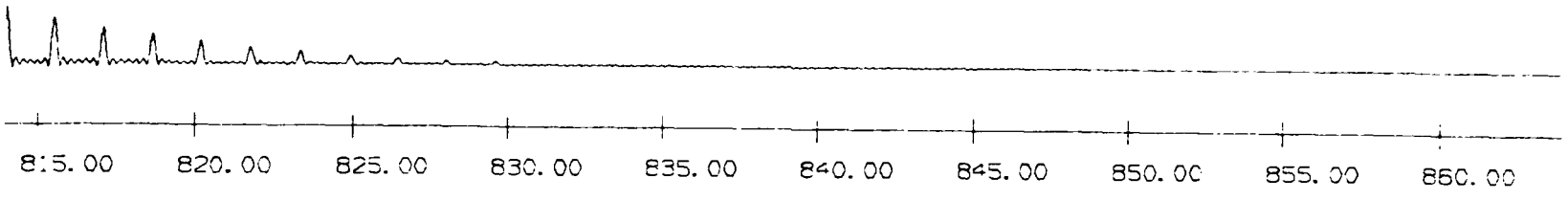
815.00
820.00
825.00
830.00
835.00
840.00
845.00
850.00
855.00
860.00

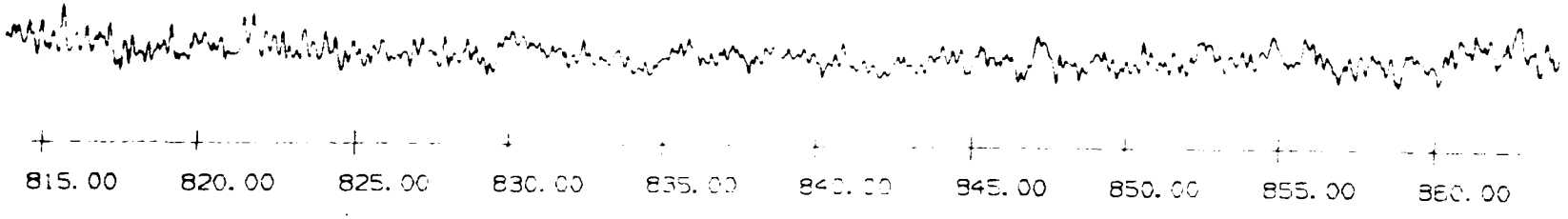
815.00
820.00
825.00
830.00
835.00
840.00
845.00
850.00
855.00
860.00

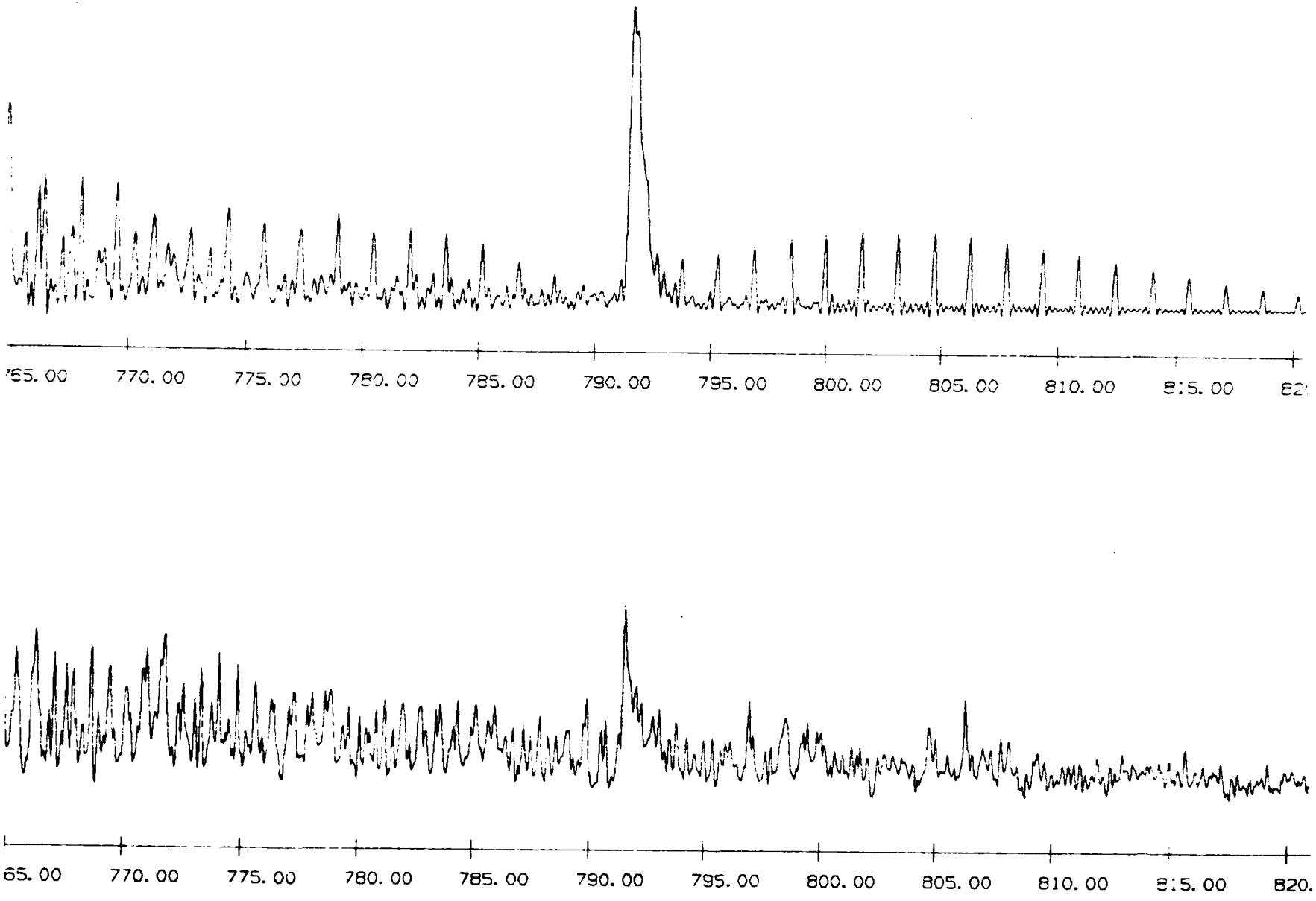
765.00
770.00
775.00
780.00
785.00
790.00
795.00
800.00
805.00
810.00
815.00
820.
WAVE NUMBER

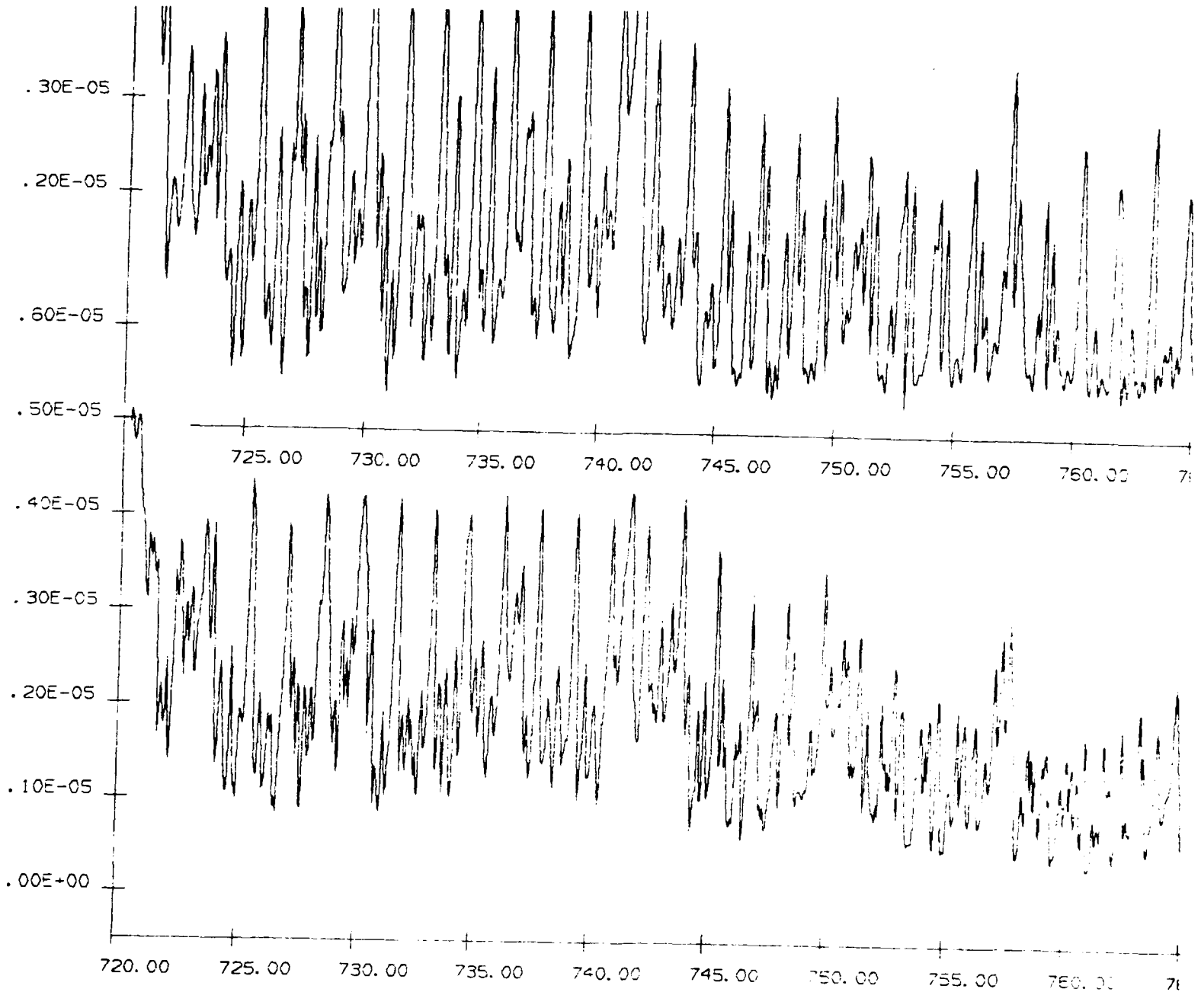
.30E-05
.20E-05
.60E-05
.50E-05
.40E-05
.30E-05
.20E-05
.10E-05
.00E+00
725.00
730.00
735.00
740.00
745.00
750.00
755.00
760.00
720.00
725.00
730.00
735.00
740.00
745.00
750.00
755.00

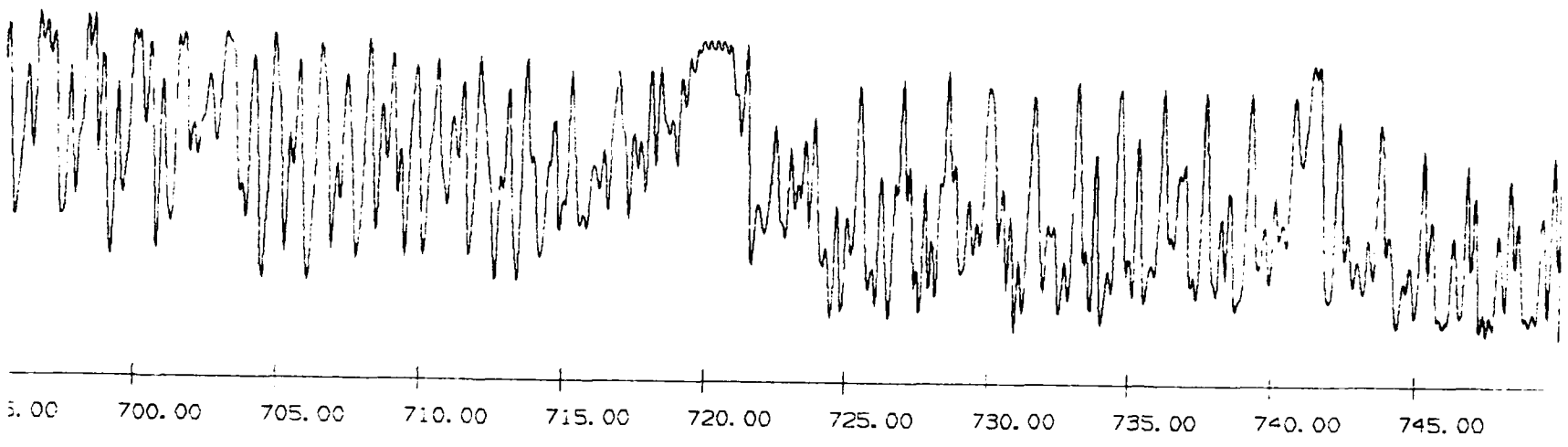
5.00
700.00
705.00
710.00
715.00
720.00
725.00
730.00
735.00
740.00
745.00

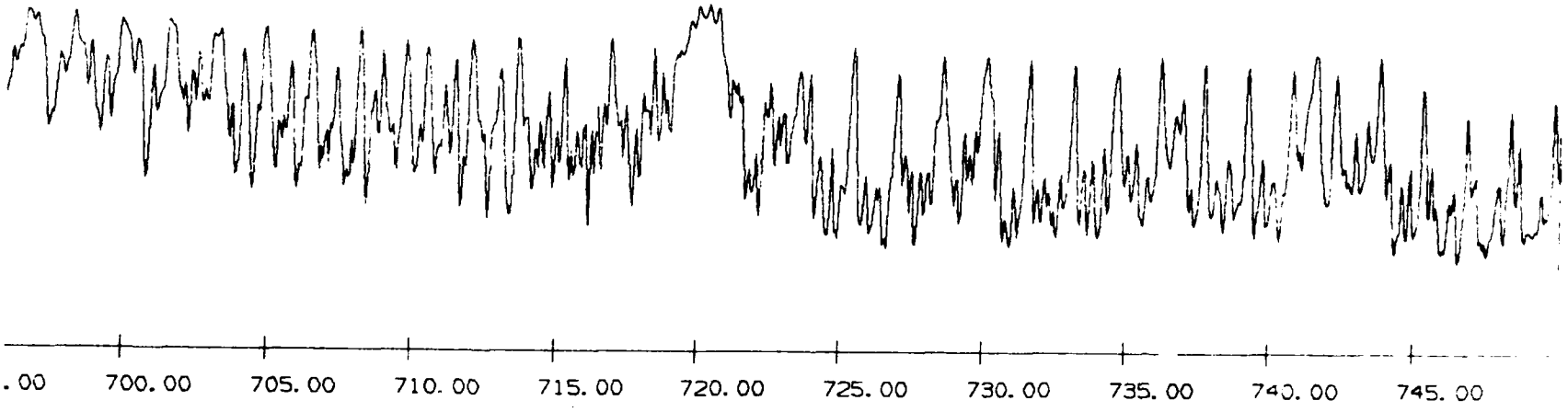
.00
700.00
705.00
710.00
715.00
720.00
725.00
730.00
735.00
740.00
745.00

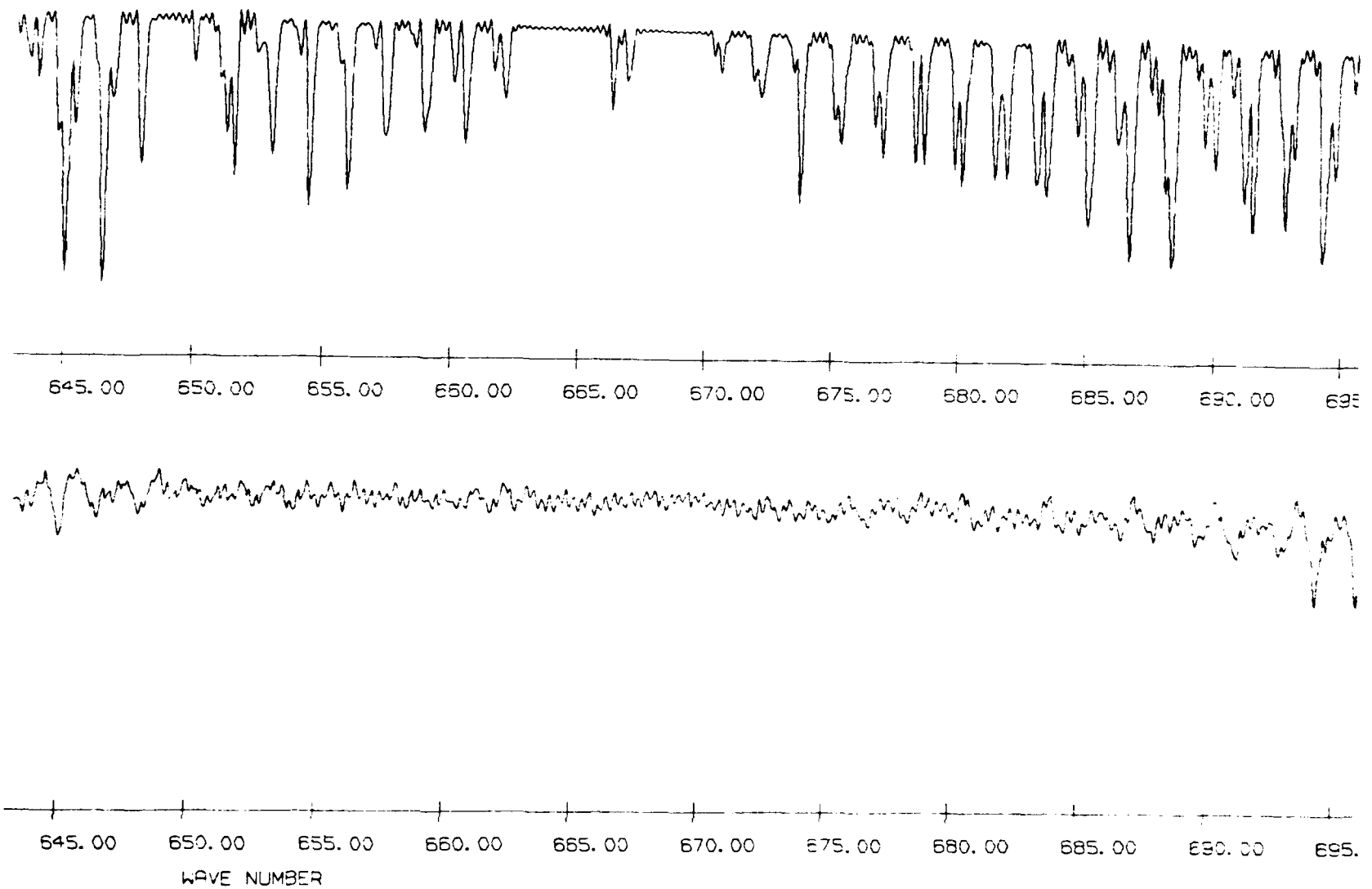
645.00
650.00
655.00
660.00
665.00
670.00
675.00
680.00
685.00
690.00
645.00
650.00
655.00
660.00
665.00
670.00
675.00
680.00
685.00
690.00
695.
WAVE NUMBER

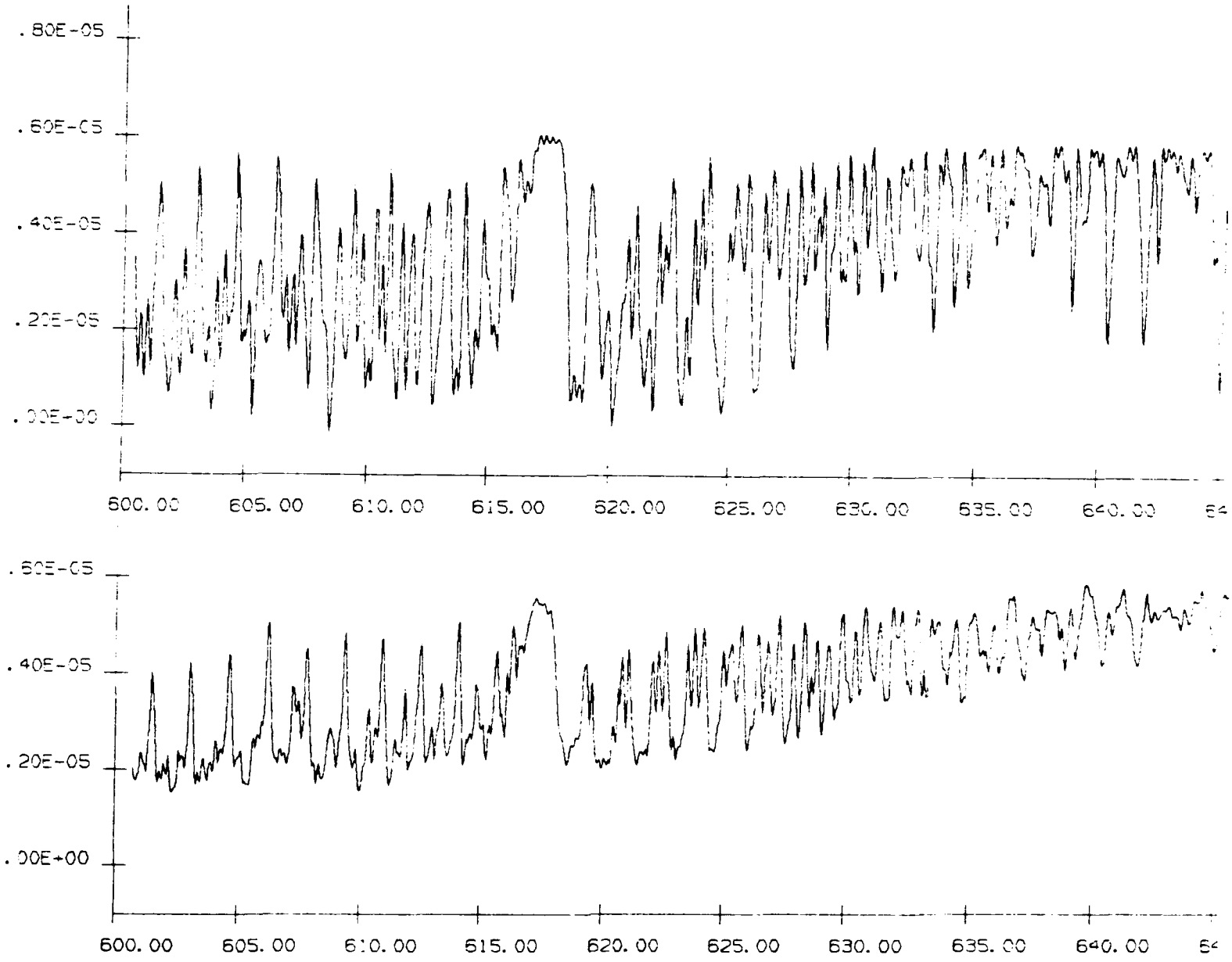
.80E-05
.60E-05
.40E-05
.20E-05
.00E+00
600.00
605.00
610.00
615.00
620.00
625.00
630.00
635.00
640.00
.60E-05
.40E-05
.20E-05
.00E+00
600.00
605.00
610.00
615.00
620.00
625.00
630.00
635.00
640.00

Figure 51

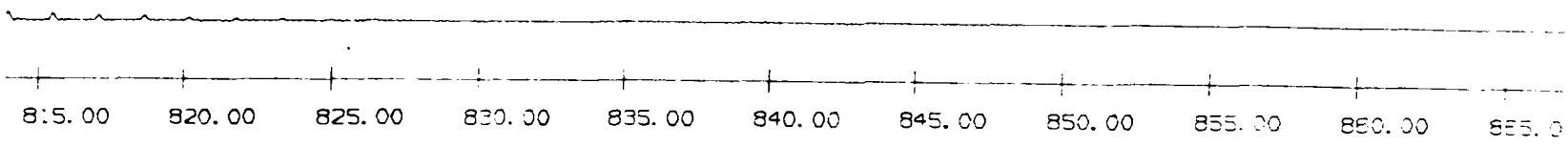
815.00
820.00
825.00
830.00
835.00
840.00
845.00
850.00
855.00
860.00
865.0

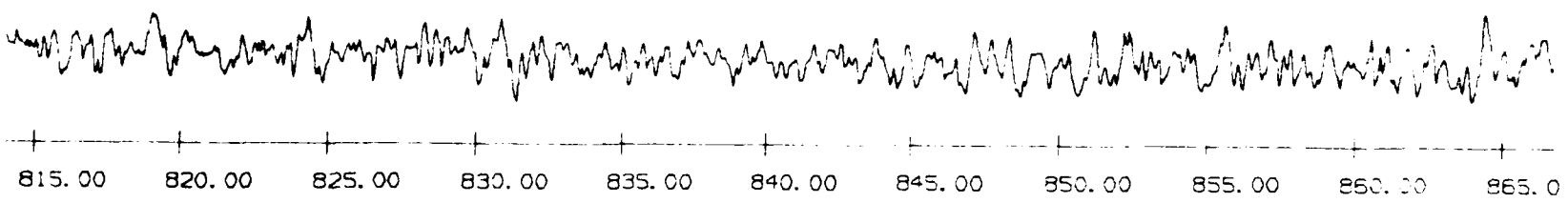
815.00
820.00
825.00
830.00
835.00
840.00
845.00
850.00
855.00
860.00
865.0

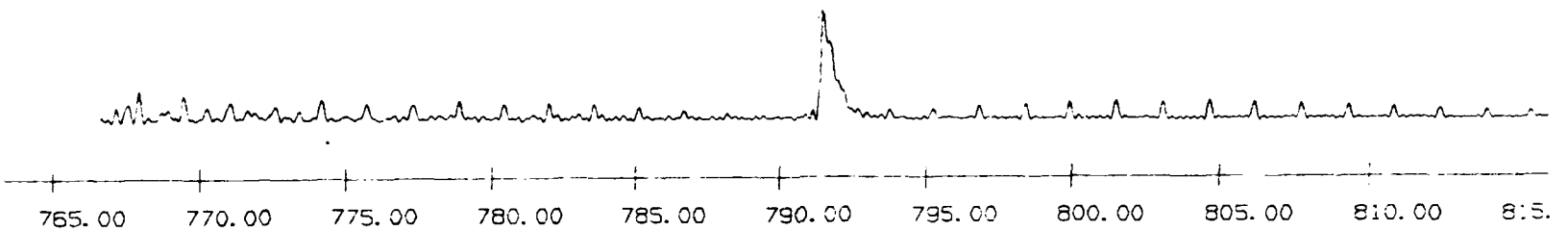
765. 00
770. 00
775. 00
780. 00
785. 00
790. 00
795. 00
800. 00
805. 00
810. 00
815.

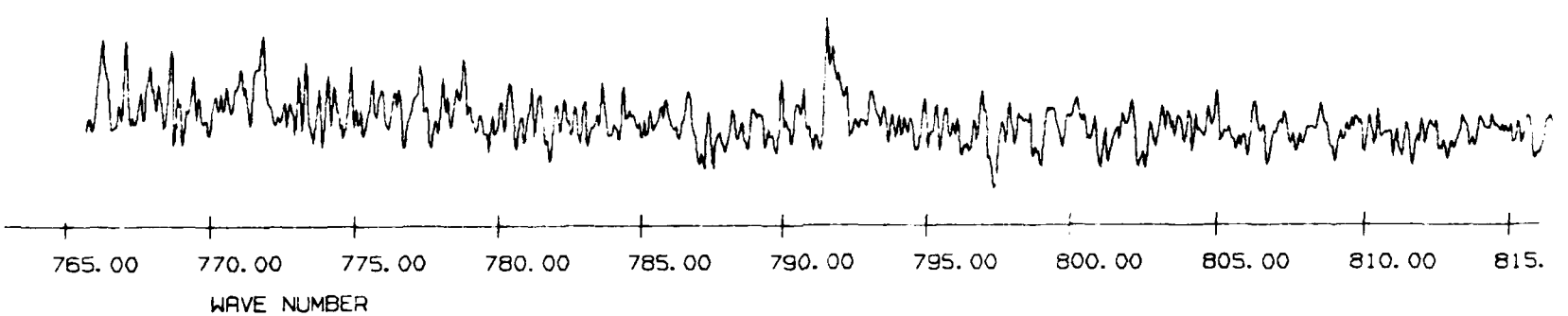
765. 00
770. 00
775. 00
780. 00
785. 00
790. 00
795. 00
800. 00
805. 00
810. 00
815.
WAVE NUMBER

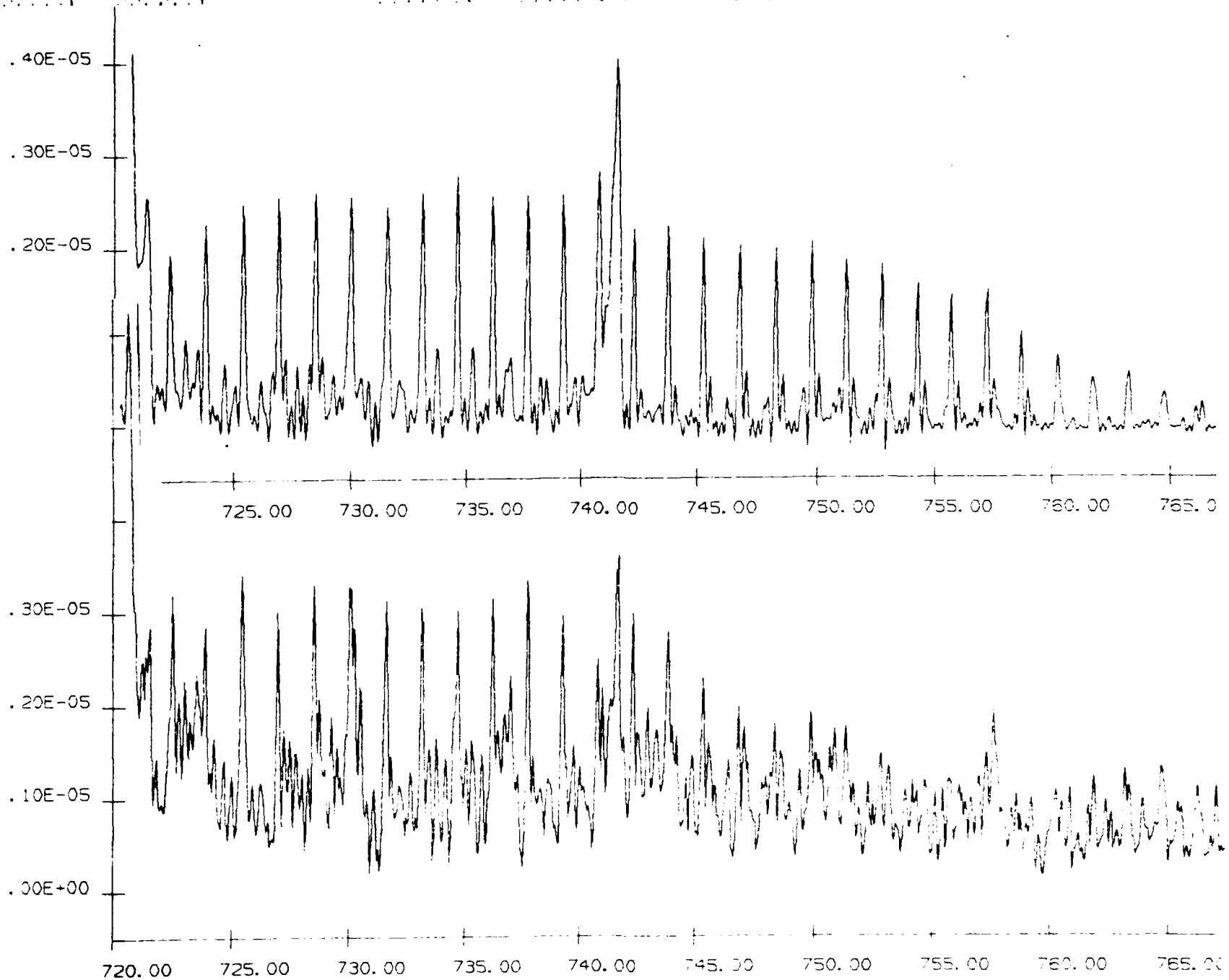
.40E-05
.30E-05
.20E-05
725.00
730.00
735.00
740.00
745.00
750.00
755.00
760.00
765.0
.30E-05
.20E-05
.10E-05
.00E+00
720.00
725.00
730.00
735.00
740.00
745.00
750.00
755.00
760.00
765.00

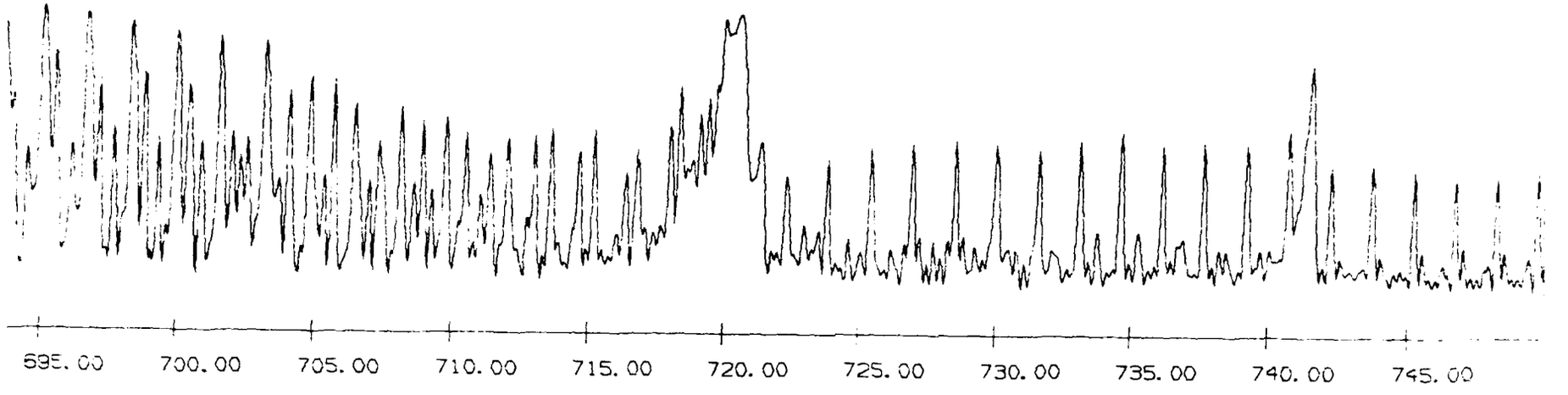
695. 00
700. 00
705. 00
710. 00
715. 00
720. 00
725. 00
730. 00
735. 00
740. 00
745. 00

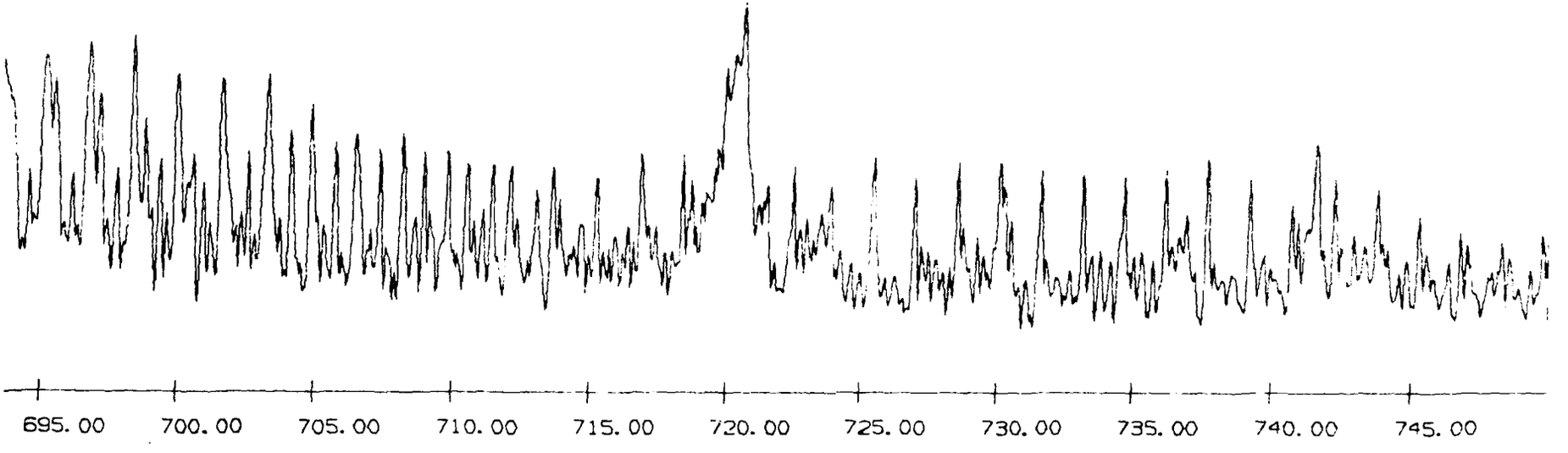
695. 00
700. 00
705. 00
710. 00
715. 00
720. 00
725. 00
730. 00
735. 00
740. 00
745. 00

END

FILMED

7-85

DTIC